

Approximation, torsion, and amodally-completed surfaces

C. Fantoni^{a,*}, W. Gerbino^a, P.J. Kellman^b

^a *Department of Psychology and B.R.A.I.N. Center for Neuroscience, University of Trieste, via Sant'Anastasio 12, 34134 Trieste, Italy*

^b *Department of Psychology, University of California, Los Angeles, 405 Hilgard Avenue, Los Angeles, CA 90095-1563, USA*

Received 29 December 2006; received in revised form 25 January 2008

Abstract

Consider a stereoscopic display simulating two rectangular patches, the lower frontoparallel and the upper slanted around the vertical axis. When the two patches are amodally-completed and appear as the unoccluded parts of a smooth surface partially hidden by a foreground frontoparallel surface, either real or illusory, their relative slant is underestimated with respect to a baseline condition in which they are perceived as separate rectangles. Slant assimilation was studied in three experiments using with- vs. without-occluder displays and two methods, slant matching and speeded classification of twist direction. In Experiments 1 and 2 we found slant assimilation in with-occluder displays and slant contrast in without-occluder displays. In Experiment 3 we isolated a component of slant assimilation attributable to the mere presence of the occluder. Twist classification performance was impaired even when edge geometry hindered amodal completion, but the performance loss was larger when surface patches were amodally completed. To minimize the required amount of torsion, input fragments are misperceived, indicating that in limiting conditions amodal completion is mediated by approximation rather than interpolation. Slant assimilation decreases as twist angle increases, up to a limit above which the visual system does not support the formation of a smooth amodal surface with torsion.

© 2008 Elsevier Ltd. All rights reserved.

Keywords: Amodal completion; Visual interpolation; Visual approximation; Torsion; Good continuation; 3D shape

1. Introduction

Fig. 1 illustrates an effect of amodal completion on perceived slant specified by horizontal scale disparity of untextured patches, as originally discussed by Fantoni, Gerbino, and Kellman (2004, 2005). The perceived twist is *smaller* in the left stereogram (where the gray patches are amodally completed into a unitary surface with torsion) than in the right stereogram (where they are perceived as separated surfaces). Liu and Schor (2005) discussed our effect, labeled it *slant assimilation*, and conducted three experiments using other displays. Their stereograms simulated three vertically-aligned planar patches specified by random dots and slanted about the vertical axis, including two semi-circular patches (equally slanted about the vertical) and a cen-

tral elliptical test patch of variable slant. In the with-occluder condition observers underestimated the stereoscopic slant difference between the central test (visible in an aperture of the occluder) and the reference patches, relative to the without-occluder condition.

The slant assimilation effect observed in Fig. 1 cannot be attributed to the occluder as a proximal frame of reference for the horizontal scale disparity of the upper patch, since the superiority of relative over absolute disparity runs in the opposite direction (Gillam & Blackburn, 1998; Gillam, Flagg, & Finlay, 1984; Gillam & Pianta, 2005; Van Ee & Erkelens, 1995; Wallach & Lindauer, 1962). Nor can it be attributed to the conflict between disparity (indicating slant) and the lack of perspective (indicating no slant), since the latter is more evident in without-occluder than with-occluder displays (Clark, Smith, & Rabe, 1956; Cutting & Millard, 1984; Freeman, 1966; Gillam, 1968; Stevens & Brookes, 1988; van Ee, van Dam, & Erkelens, 2002).

* Corresponding author. Fax: +39 0404528022.

E-mail addresses: fantoni@psico.units.it (C. Fantoni), gerbino@units.it (W. Gerbino), Kellman@cognet.ucla.edu (P.J. Kellman).



Fig. 1. Amodal completion modulates the amount of perceived slant from horizontal scale disparity (Fantoni et al., 2004). As shown in the upper diagrams, divergers should free-fuse the leftmost stereogram pair and cross fusers the rightmost pair in each triplet. The perceived slant is *smaller* on the left than on the right.

Here we report three experiments on untextured patches like those in Fig. 1. Such experiments complement the work by Liu and Schor (2005) and address further issues, for the following reasons. First, the amodal completion of two patches into a surface with a single twist is more elementary than the amodal completion of three patches into a surface with two twists. Second, our rectangular patches provide less slant-from-shape information than Liu and Schor's circular patches. Third, Da Vinci stereopsis is not involved in our displays (no vertical occluding contours), while it is present in Liu and Schor's with-occluder displays. Fourth, the comparison of with- vs. without-occluder conditions is balanced in our displays (where Da Vinci stereopsis is never involved), while it is unbalanced in Liu and Schor's displays (where Da Vinci stereopsis is involved only in the with-occluder condition).

We found slant assimilation in displays with an occluder specified by either luminance borders (Experiment 1) or illusory borders (Experiment 2), as well as a consistent loss of slant discrimination in an objective classification task (Experiment 3). Such findings do not fit the hypothesis that amodal completion is mediated by the *visual interpolation* of literally-represented fragments; i.e., contour segments and surface patches whose perceived positions and orientations match those locally specified in the input. Rather, they fit the hypothesis that amodal completion is mediated by *visual approximation*, a process that minimizes the required amount of surface torsion and generates a smooth surface including modal parts that do *not* match input patches, when they approach the geometric limits embodied in visual completion models. The next two sections describe how an approximation-based approach to amodal completion can provide a functional account of slant assimilation compatible with neural mechanisms evoked by Liu and Schor (2005) to explain the top-down influence of perceptual grouping.

2. Conditions for 2D and 3D completion

Visual completion captures the idea that perception goes beyond point-by-point correspondences with local stimulus information (Kanizsa & Gerbino, 1982; Kellman & Shipley, 1991; Koffka, 1935; Marr, 1982; Metzger, 1954; Michotte, Thinès, & Crabbé, 1964). We utilize it to label a set of percep-

tual phenomena, while “interpolation” and “approximation” indicate alternative processes underlying the formation of a unitary representation of input fragments.

The typical stimulus for contour completion is a pair of T-junctions with *tangent discontinuities* between top and stem contours (Shipley & Kellman, 1990). The geometric constraints describing the set of spatial relations required for the perception of a single contour from a pair of separated junction stems are formalized by *contour relatability* (Kellman & Shipley, 1991). In 2D conditions two junction stems are relatable when their connection bends in only one direction (monotonicity constraint) through an obtuse angle (90-deg constraint). Physiological and psychophysical studies favor a graded relatability notion, involving the fast continuous decay of completion strength beyond relatability limits, rather than an all-or-none notion (Kellman & Shipley, 1991). Suboptimal relatability affects both salience (Kellman & Shipley, 1991; Sha'shua and Ullman, 1988; Singh & Hoffman, 1999) and shape of perceptually completed contours (Fantoni, Bertamini, & Gerbino, 2005; Fantoni & Gerbino, 2003; Gerbino & Fantoni, 2006). As regards the monotonicity constraint, subjective estimates (Shipley & Kellman, 1992; Tse, 1999a), objective performance measures (Kellman, Yin, & Shipley, 1998; Mussap & Levi, 1995; Takeichi, Nakazawa, Murakami, & Shimojo, 1995), and physiological evidence (Fiorani, Rosa, Gattas, & Rocha-Miranda, 1992; Li & Li, 1994) confirmed that visual completion tolerates misalignments of parallel junction stems less than 15–20 min of arc (Hilger & Kellman, 2005; Roncato & Casco, 2003; Shipley & Kellman, 1992). As regards the 90-deg constraint, visual completion has been studied in patterns including partially occluded angles smaller than 90 deg (Fantoni & Gerbino, 2001; Guttman, Sekuler, & Kellman, 2004).

A general theory of completion should also cover the 3D domain (Kellman, 2003; Saidpour, Braunstein, & Hoffman, 1994; Yin, Kellman, & Shipley, 1997, 2000), as demonstrated by effects on 3D positions and orientations of edges. Kellman, Garrigan, Yin, Shipley, and Machado (2005b) tested different amounts of misalignment of 3D-relatable surface patches and found that even small misalignments substantially weakened completion effects. Recent work indicates that similar effects occur also in the absence of explicit edge information and depends on geometric con-

straints for surface patches that parallel those for contours (Fantoni, Hilger, Gerbino, & Kellman, submitted for publication). As proposed by Kellman, Garrigan, and Shipley (2005), reliability can be generalized to the 3D case, with both reliability constraints applying in a graded fashion.

Relative to 2D reliability, 3D reliability implies a broader class of limits. 2D reliability is violated only in three cases: (a) misaligned and parallel fragments; (b) fragments converging at an angle ≤ 90 deg; (c) any combination of a and b. 3D reliability is violated in 15 cases, corresponding to all combinations of the following four patterns of surface patches, each occurring in isolation or together with any other: (1) depth misalignment; (2) misalignment in the image plane; (3) opposite inclination around the horizontal axis, beyond the 90-deg constraint; (4) twist around the vertical axis (Fig. 2). Any elastic 3D connection of surface patches in (1) and (2) would generate an *inflected* surface with null total curvature variation in depth as well as in the image plane; pattern (3) would involve the generation of a *curved* surface with total curvature variation in depth lower than 90 deg; while pattern (4) would involve the generation of a surface with *torsion*. The completion of patches corresponding to different combinations of the four basic patterns would generate surfaces characterized by different combinations of inflection, curvedness, and torsion.

While inflection and curvedness are common to both 2D and 3D completion, torsion is specific to the 3D domain and constitutes an intriguing, yet inadequately explored, property of amodally-completed 3D surfaces. In general, little attention has been devoted to completion by curved surfaces. Notable exceptions are studies on bending of stereoscopic surfaces (Zanforlin, 1982), phenomenal undulation (Massironi & Sabin, 1983), phenomenal folding (Massironi, 1988), smooth twisting with torsion (as in the worm pattern by Tse, 1999b, Fig. 11, and modified Kanizsa square by Kellman, Garrigan, & Shipley, 2005, Fig. 22).

3. Visual interpolation and visual approximation

The notion of approximation, which we apply here to amodal completion, comes from statistics and computation. It arises, for example, in curve fitting, as discussed by Ullman (1996, pp. 141–143). Consider the problem of fitting a polynomial function to a generic arrangement of n points: interpolation describes the case in which the curve goes exactly through all n points, while approximation

describes the case in which the curve passes near but not exactly through the points. Approximation provides a non-literal representation of the input, involving an error that increases as the degree of the fitting function decreases, but can effectively account for noisy data. When the arrangement of the n points is singular (e.g., four points along a parabolic path), the degree of the interpolating function can be less than $(n - 1)$: in these cases interpolation and approximation can coincide.

Following such a distinction one can contrast two models of contour fragment completion: the interpolation of a missing contour that joins the literal representations of two junction stems and the approximation of a missing contour that (in general) joins their non-literal representations. Ordinarily, completion has been modeled by interpolation (Horn, 1981; Kellman & Shipley 1991; Ullman, 1976; see Fantoni & Gerbino, 2003 for a review of models). However, when the geometry of junction stems gets to the limits of reliability, interpolation- and approximation-based solutions do differ and can be matched to empirical data.

At the theoretical level, the emergence of approximation-based solutions is consistent with the optimization of stimulus conformity (Rock, 1983, chapter 5) and of the complexity of amodal parts. Stimulus conformity can be defined as the reciprocal of the amount of discrepancy between approximated and image-specified positions and orientations of junction stems: while the complexity of amodal parts can be defined as a function of several variables, including closure, total squared curvature (Sha'shua & Ullman, 1988), and convexity (Feldman & Singh, 2005; Pao, Geiger, & Rubin, 1999). At the level of underlying processes, approximation might result from the integration of position and orientation signals biased towards reliability.

Approximation-based effects depend on the discrepancy between image contour fragments and the modal parts of the approximated trajectory. We hypothesize that such discrepancies are always in the direction of the minimal deviation from reliability, but are phenomenally experienced in different ways according to the amount of stimulus support (Rock, 1983, chapter 5). When input evidence is poor (*weak* stimulus support) the discrepancy is not experienced because the approximated trajectory dominates; while the discrepancy is experienced as such when the mismatching input evidence is rich (*strong* stimulus support).

Cases of weak stimulus support are Fig. 1 and displays used in our experiments where the relative slant of the two

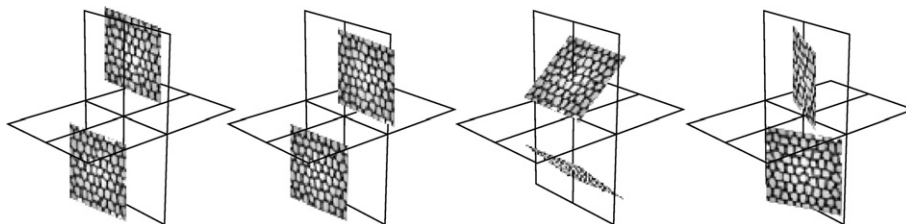


Fig. 2. Four basic patterns of two surface patches violating 3D reliability: (1) depth misalignment; (2) misalignment in the image plane; (3) opposite inclination around the horizontal axis, beyond the 90-deg constraint; (4) twist around the vertical axis.

planar patches is weakly supported by the stimulus, being specified only by horizontal scale disparity against several cues to flatness (e.g., uniform texture, lack of linear perspective). Other effects of approximation on weakly supported parts are as follows. Observers are less likely to report a Vernier offset between two bars when the depth ordering of an interposed surface is consistent with amodal completion (Mussap & Levi, 1995); small vs. large Vernier offsets between bars separated by an occluder are better discriminated than offsets between isolated bars (Gerbino, Scomersi, & Fantoni, 2006); the sensitivity to depth offset is lower for surface patches that can be completed behind an occluder than for surface patches that cannot (Hou, Lu, Zhou, & Liu, 2006; Liu, Jacobs, & Basri, 1999; Yin et al., 2000).

A case of strong stimulus support is the display shown in Fig. 3 (Gerbino, 1978). In the Gerbino illusion—so labeled by da Pos and Zambianchi (1996)—each occlusion leads to a violation of contour relatability, given that the borders of the equilateral triangles coincide with hexagon vertices. Although a tendency toward global shape regularity would support perceiving the hexagon veridically, each partially occluded angle appears distorted. Consistently with approximation, the effect includes a misorientation of the hexagon in the direction of the avoidance of the coincidental occlusion (Fantoni, Gerbino, & Rigutti, 2007).

4. Experimental hypotheses

To test the hypothesis that the completion of twisted patches involves visual approximation, we used stereograms like those in Fig. 1, and expected a relative slant underestimation in with- vs. without-occluder displays, as a measure of slant assimilation. Since the twist of surface patches likely violates relatability constraints, an approximated surface should be generated, producing slant assimilation and, consequently, a reduced sensitivity for twist direction in with- vs. without-occluder displays. The absence of slant assimilation would be inconclusive, being consistent with the literal representation of image-specified patches, either interpolated or not.

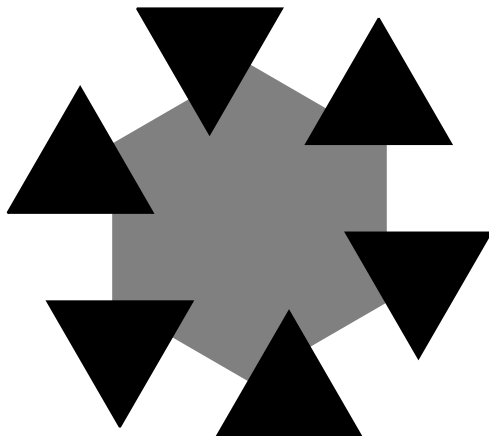


Fig. 3. The Gerbino illusion.

The amount of twist angle θ is expected to affect the shape of the approximated surface and, consequently, the amount of slant assimilation. As θ increases, the required amount of torsion increases and visual approximation becomes less likely. To predict the effect of θ we hypothesized that approximation occurs only in an interval around coplanarity defined by a critical twist value $|\kappa|$ beyond which the two patches are perceived as independent surfaces. Fig. 4 contrasts continuous (left) vs. discrete (right) variations of slant assimilation over θ , reflecting alternative models of approximation effectiveness.

The possible effect of the vertical alignment between surface patches was controlled by comparing symmetrically-aligned displays (like those in Fig. 1) and asymmetrically-aligned displays, in which the simulated depth offset doubles and one side only of the upper rectangle carries all the disparity. Smooth surfaces connecting symmetrically- vs. asymmetrically-aligned patches differ in the distribution of torsion along the central horizontal meridian (i.e., the line in the middle of the gap between the two patches). In symmetrically-aligned displays torsion is half negative and half positive, being minimal/maximal at the endpoints of the meridian and null at the center. In asymmetrically-aligned displays torsion is null at the endpoint with zero disparity and wholly negative or positive, depending on twist direction, reaching either the minimum or the maximum at the other endpoint. If approximation depends on extremal torsion, slant assimilation should be weaker in symmetrically-aligned displays (low extremal torsion) than asymmetrically-aligned displays (high extremal torsion). By contrast, if approximation depends on the overall amount of torsion, slant assimilation should be equal in the two types of displays.

We tested these expectations in three experiments. In Experiments 1 (with vs. without a real occluder) and 2 (with vs. without an illusory occluder) we used a slant matching paradigm and measured the perceived slant of the upper patch in stereoscopic displays similar to those in Fig. 1, but with an including square window that provided the reference for disparities of the frontoparallel occluder and gray patches. In the absence of texture, the relative depth of the occluding rectangle was specified by identical horizontal displacements of the two vertical sides, while the relative slant of the two gray patches was specified by their different widths in the left/right images. In Experiment 3 we used a speeded classification of twist direction and measured twist sensitivity, again comparing with- vs. without-occluder displays.

5. Experiment 1: Relative slant with vs. without a real occluder

5.1. Method

5.1.1. Participants

Forty-seven undergraduate students of the University of Trieste with normal or corrected-to-normal vision and naive to the purpose of the experiment served as unpaid

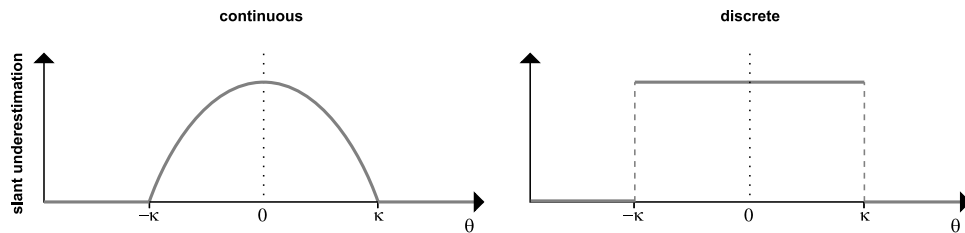


Fig. 4. Amount of slant underestimation in with- vs. without-occluder displays as a function of the twist angle θ , according to a continuous (left) vs. discrete (right) model of approximation.

participants. Eight participants were omitted from the experimental session because they failed the screening test for stereoscopic vision, while three of the 39 observers who completed the experimental session were excluded from the final analysis due to failure to meet the threshold criterion for performance in the experimental task (average individual scores should fall between 1.96 and $-1.96 z$ points). Observers were randomly assigned to one of the two levels of the between-subjects factor of presence or absence of the occluder.

5.1.2. Apparatus and displays

Stereograms were displayed on a LG StudioWorks 775E CRT screen set at the 1024×768 pixel resolution, driven by a COMPAQ Deskpro. Stimuli were presented by means of a Matlab program using PsychToolbox functions (Pelli, 1997). Displays were image pairs viewed through a double mirror stereoscope, centered on the middle of the screen and located at a distance of 44 cm (Fig. 5). The effective distance from the pupil to the center of a monocular image was 50 cm. The centers of the two monocular images were 15-cm apart. The four high-quality front surface mirrors composing the stereoscope were adjusted to a fixed interocular distance of 6.5 cm and null vergence angle. At this distance a pixel subtended approximately 2 min of arc.

Stimulus parameters are depicted in Fig. 6. The stereograms included a white (75 cd/m^2) square window with 6.3-deg sides, bordered by a black field filling the entire screen, and two medium-gray (24 cd/m^2) vertically-aligned rectangles separated by either a 0.7-deg gap in the without-occluder condition or a black (3 cd/m^2) occluder ($0.70 \times 4.25 \text{ deg}$) with 0.56-deg crossed disparity in the with-occluder condition. In monocular images the upper side of the upper rectangle and the lower side of the lower rectangle were juxtaposed to the black field surrounding the white window.

In all stereograms the upper and lower gray patches simulated equal rectangular laminas, 2.8-deg high. The lower patches, simulating a frontoparallel lamina, were 1.8-deg wide in both monocular images and had zero disparity relative to the white window. To manipulate the slant of the upper lamina we reduced the width of one monocular patch relative to the other, producing a horizontal scale disparity. The widths of left and right-upper patches were calculated as being $W_{l,r} = W \cos(\theta \pm \beta/2)$; where W is the

projected width of the frontoparallel patch seen by the cyclopean eye and $\beta = 2 \text{ atan}(h/d)$, with h the interocular distance and d the distance of the center of the patch from the cyclopean eye. As shown in Fig. 7 top, the following six amounts of relative slant θ were used: $-30, -20, -10, 10, 20, 30 \text{ deg}$ (relative to $h = 3.25 \text{ cm}$ and $d = 50 \text{ cm}$). The horizontal scale disparities of the upper patches were 2.37 min when $\theta = \pm 10 \text{ deg}$, 4.70 min when $\theta = \pm 20 \text{ deg}$, and 6.85 min when $\theta = \pm 30 \text{ deg}$, corresponding to horizontal magnifications of 2.4%, 5.0%, and 8.0% of either the left or right patch, depending on the slant sign (negative when the left side was closer to the observer and positive in the opposite case).

Symmetric displays were obtained by assigning the same amount of disparity to the left and right sides of upper patches, so that the amounts of crossed disparity of one

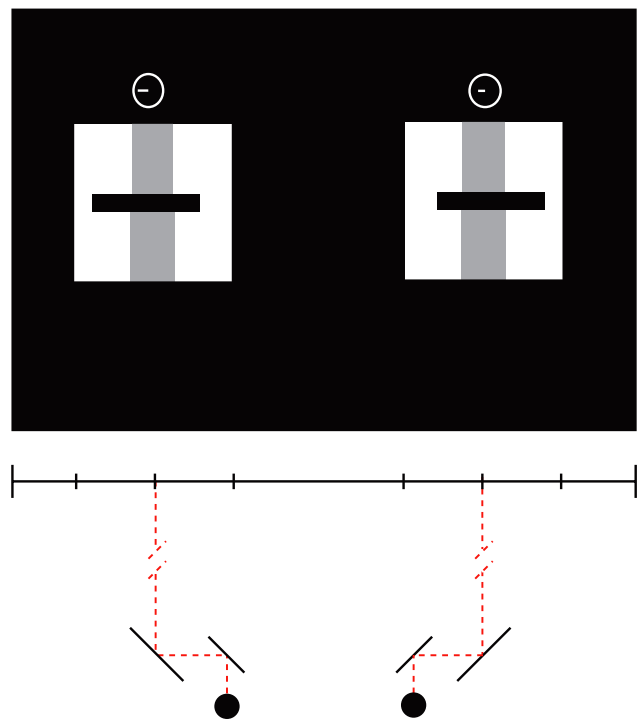


Fig. 5. Above, a representative stereogram used in Experiment 1, illustrating a symmetric with-occluder display with 30-deg twist and the upper gauge probe. Below, a diagram of the stereoscopic viewing apparatus, including four mirrors that allowed observers to fuse left and right images simultaneously displayed on a CRT screen; dashed lines show the monocular axes for a standard observer with an interocular distance of 6.5 cm.

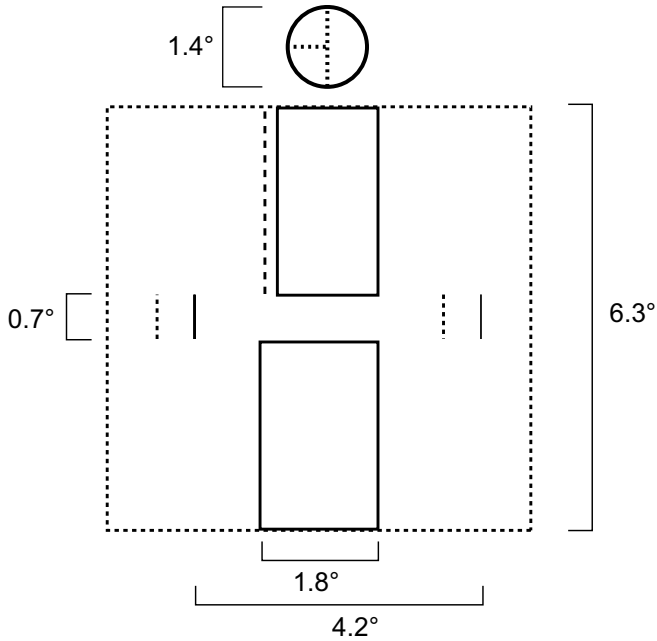


Fig. 6. The diagram illustrates vertical/horizontal extents for the asymmetrically-aligned with-occluder display with relative slant $\theta = -30$ deg; continuous lines depict the left-eye and dashed lines the right-eye image (see text for disparity measures).

side and uncrossed disparity of the other were equal. In this condition upper and lower patches were horizontally center-aligned in both monocular images. Asymmetric displays were obtained by assigning the full amount of disparity to one side of the upper patch and zero disparity to the other; upper and lower patches were right-side aligned in half asymmetric displays and left-side aligned in the other half. We strived to optimize slant perception by locating the slant axis of the upper surface at the same depth level of the surrounding black field. Several studies (Gillam, Chambers, & Russo, 1988; Kaneko & Howards,

1996; Pierce & Howards, 1997; van Ee & Erkelens, 1995) have demonstrated that a slanted surface above or below a frontal surface supports the immediate and nearly veridical perception of slant, despite conflicting cues.

The monocular images included a set of T-junctions consistent with the perception of upper and lower rectangular patches amodally continuing behind the surrounding black field. With respect to Fig. 1, the addition of the surrounding black field (a) provided a reference level for the depth of the untextured occluder, (b) prevented a possible conflict with linear perspective, given that in any polar projection the top side of the slanted upper rectangle would be oblique, and (c) introduced an imbalance between the positive vs. negative slant of asymmetrically-aligned patches, in which T-junctions were consistent with an upper rectangle slanting away from (but not towards) the observer. As regards (c), we hypothesized that such an imbalance might produce a selective effect of slant direction in asymmetric displays alone.

The without-occluder condition illustrated in Fig. 7 bottom right was used to control for possible effects unrelated to amodal completion, like the effect of viewing distance (Johnston, 1991) and the slant contrast between twisted laminas (Gillam & Blackburn, 1998; Gillam & Pianta, 2005).

Since the upper patch was a horizontally-compressed copy of the bottom patch, we also controlled for relative width as a foreshortening cue to unsigned slant (Gillam, 1968; Hillis, Watt, Landy, & Banks, 2004; Stevens, 1981; van Ee et al., 2002; Youngs, 1976), including in each alignment condition three additional stereograms with identical monocular upper rectangles. This manipulation removed disparity information for slant while preserving relative width as a pictorial cue, thus providing a baseline for slant-from-disparity measures. The widths of the baseline upper rectangles were 1.51, 1.65, and 1.73 deg for $\theta = \pm 30, \pm 20$, and ± 10 deg, respectively. Relative to the

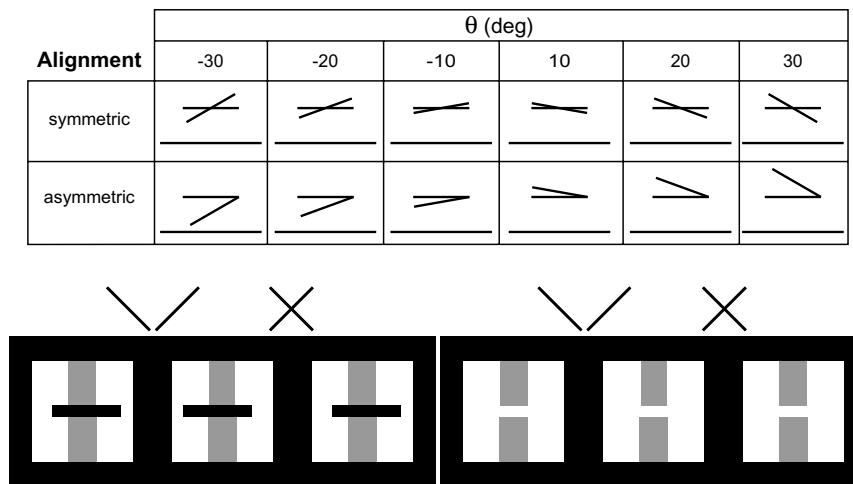


Fig. 7. Stimuli used in Experiment 1. The upper table shows the top view of the simulated 3D patterns (two patches plus occluder) in the 12 conditions (6 relative slants \times 2 alignments); in all conditions the lower patch and the surrounding black field had the same disparity. The lower stereograms depict with-occluder (left) and without-occluder (right) symmetric displays with $\theta = 30$ deg.

width of 1.8-deg lower rectangle, the horizontal compressions were 16%, 8%, and 4%.

In every trial the observer provided a measure of the perceived slant of the upper patch by adjusting the slant of a white-outline gauge probe that simulated a 1.4-deg circle with a 0.7-deg normal line stacked on its center, displayed along the central vertical axis 21 min above the upper side of the square window. The slant of the gauge probe was controlled by leftward/rightward mouse shifts that horizontally scaled the two monocular circles, transforming them into vertically-elongated ellipses: a leftward mouse shift generated a negative stereo slant, and vice versa. The gauge probe slant ranged from -85 deg (5.4 min of crossed disparity in charge to the left side of the circle) to $+85$ deg (5.4 min of uncrossed disparity in charge to the right side of the circle). The program controlled the initial slant of the gauge probe, setting it to a random orientation within the following ranges: ± 30 deg from the simulated slant of the upper rectangle for experimental displays and ± 60 deg from the frontoparallel plane for baseline displays.

5.1.3. Procedure and design

The experiment was run in a dark room allowing for dark adaptation, where participants were tested individually. The participant was seated in front of the CRT screen with his/her head stabilized by a chin rest that help maintaining the eyes at a constant distance (≈ 1.7 cm) from the ocular mirrors of the stereoscope. After instructions participants were screened for stereo vision. Only observers meeting the screening standards were given the training and experimental sessions (lasting 40 min).

5.1.3.1. Instructions. The experimenter introduced binocular vision and informed the participant that he/she would be shown simple 3D figures by means of a mirror stereoscope. Participants were encouraged to take breaks if necessary and to keep both eyes open when watching the displays.

5.1.3.2. Test for stereo vision. Participants were screened for stereo acuity using two different series of stereograms: the first series depicted a gray dihedral angle of variable size (100, 120, and 140 deg) and convexity (vertex towards vs.

away from the observer) in frontal view; the second series resembled the experimental display and depicted two patches with a 40-deg twist about the vertical, separated by either a gap or a frontoparallel occluder (depending on the group) and with variable slant direction (positive vs. negative) and alignment (symmetric vs. asymmetric). In both series participants were first asked to describe the percept by words and then to indicate the convexity of the angle (first series) or the direction of slant (second series). Participants who failed one or more times to detect either the simulated convexity of the dihedral angle or the simulated direction of slant of the upper patch did not enter the training and experimental sessions.

5.1.3.3. Training. To become familiar with the task, observers performed a training session of 18 trials in which the two sets of displays (experimental and baseline) were presented in a random order. In each trial the observer was required to verbalize the perceived direction of slant and only then to adjust the slant of the gauge probe until it appeared to run parallel with the upper rectangle.

5.1.3.4. Experimental session. The experimental session included the random presentation of 72 trials (4 repetitions of 12 experimental displays and 6 baseline displays). As shown in Fig. 8, any slant-matching trial included the following: (i) 5-s display presentation; (ii) additional presentation of the gauge probe until the observer completed his/her adjustment by pressing the right button of the mouse; (iii) 1-s blank interval before the presentation of the successive trial.

The 12 experimental displays resulted from the combination of six relative slants of the upper surface patch by two patch alignments (symmetric vs. asymmetric). The overall experiment followed a mixed factorial design with Slant Amount (3), Slant Direction (2), and Alignment (2) as within-subjects factors and Occluder (2) as a between-subjects factor.

5.2. Results

To evaluate the effects of relative width on perceived slant, we performed a preliminary analysis of mean slant estimates for baseline displays with zero horizontal scale

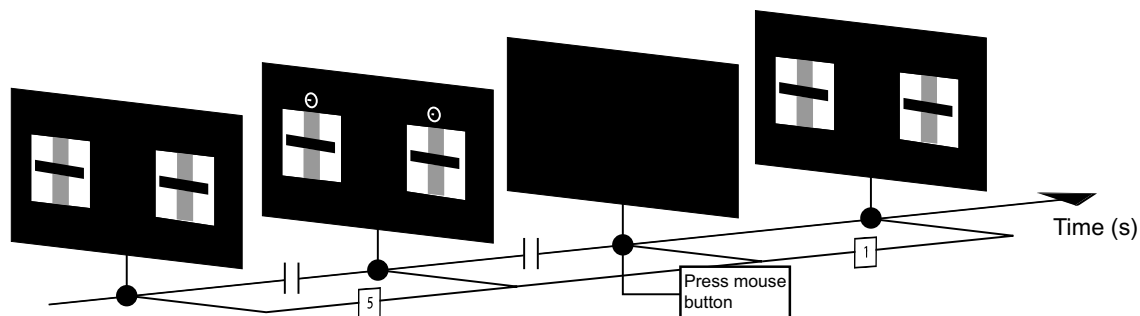


Fig. 8. Temporal sequence of events included in any trial of Experiment 1. Displays refer to the with-occluder condition.

disparity. An analysis of variance with Width (3) and Alignment (2) as within-subjects factors and Occluder (2) as a between-subjects factor showed that only the main effect of Width was significant ($F_{2,68} = 3.57, p < 0.05$). Apparently, neither the presence of a frontoparallel occluder nor the alignment of the two rectangles affected slant estimates. The main effect of Width can be attributed to the large positive error obtained with the narrower asymmetric upper rectangle, expected on the basis of the selective effect of the combination of T-junctions and foreshortening on asymmetrically-aligned patches alone. Slant estimates for 16%, 8%, 4% horizontally-compressed upper rectangles were 4.22, -0.09, 0.02 deg for asymmetric displays, and 0.60, 0.57, 0.39 deg for symmetric displays (4.22 vs. 0: $t = 2.20, df = 35$, one-tailed, $p < 0.05$; while, for the other five contrasts: $t < 1$).

To evaluate slant assimilation, two measures were derived from the matching data: *absolute estimated slant* (AES), calculated as the trimean of four differences between the raw value of matched slant and the mean value of individual matched slant for the corresponding baseline display; *relative estimated slant* [RES = (AES - θ)/ θ], with

0 corresponding to a perfect match between AES and θ , +1 to an AES twice the θ , and -1 to an AES half of the θ .

Fig. 9 shows AES (top) and RES (bottom) values as a function of signed relative stereo slant for asymmetrically (left) vs. symmetrically (right) aligned displays.

A Slant Amount (3) \times Slant Direction (2) \times Alignment (2) \times Occluder (2) mixed factorial analysis of variance was run on RES values. The main effect of Occluder was significant ($F_{1,34} = 59.00, p < 0.001$). In without-occluder displays slant was enhanced in the direction of contrast (0.43 vs. 0: $t = 5.76, df = 17$, one-tailed, $p < 0.001$); while in with-occluder displays it was attenuated in the direction of assimilation (-0.50 vs. 0: $t = 5.85, df = 17$, one-tailed, $p < 0.001$). The main effects of Alignment and Slant Direction were not significant. However, the Alignment \times Slant Direction interaction was significant ($F_{1,34} = 5.05, p < 0.05$): as expected on the basis of T-junction information, estimated slant was affected by Slant Direction when displays were asymmetric (RES_{positive slant} = 0.06 vs. RES_{negative slant} = -0.14: $F_{1,34} = 6.88, p < 0.05$), while no effect was obtained when displays were symmetric (both RES values equal to -0.03; $F < 1$). The Slant

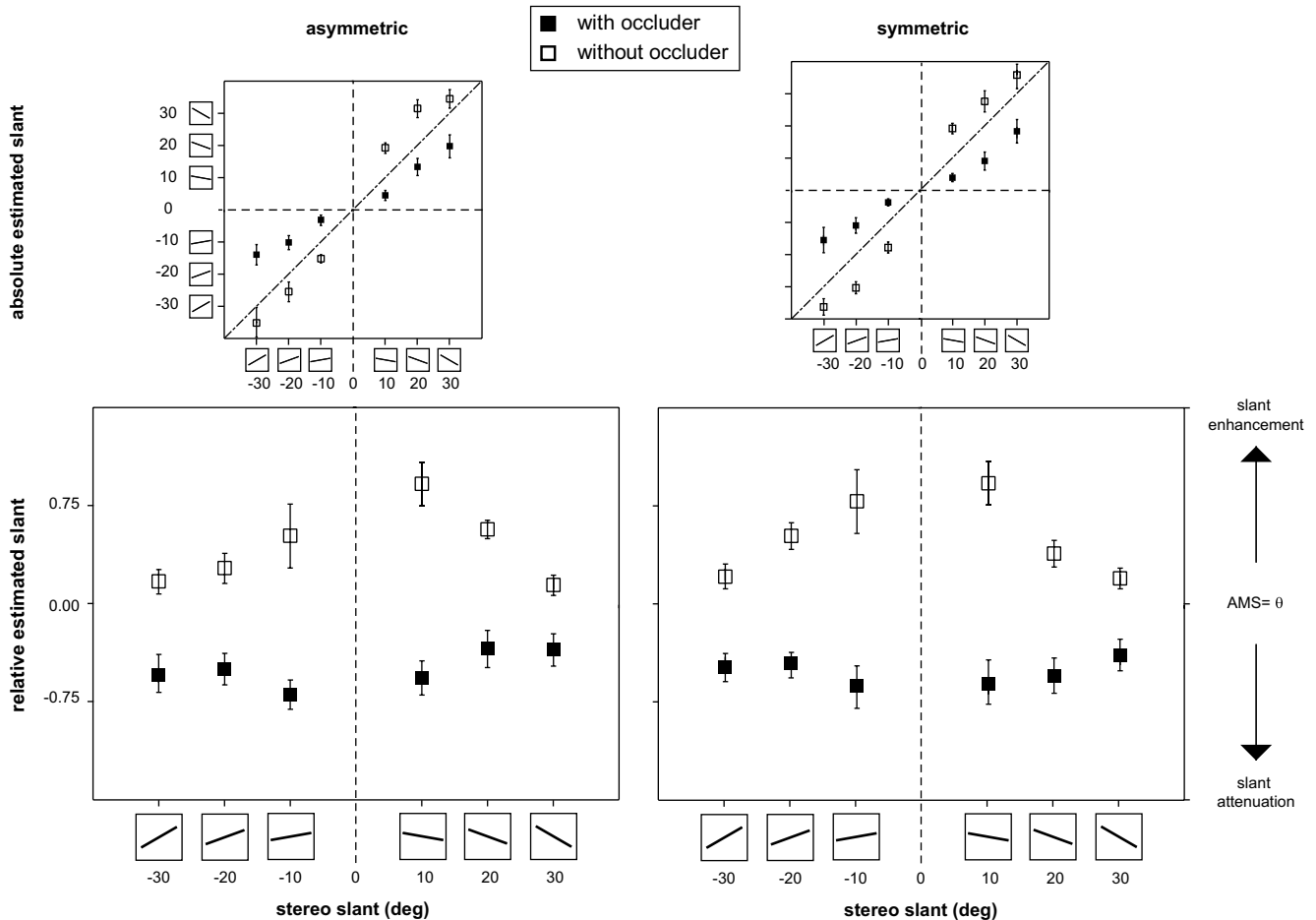


Fig. 9. Mean values of absolute estimated slant (top), and relative estimated slant (bottom), as a function of stereo slant of the upper surface patch, for asymmetrically-aligned (left) and symmetrically-aligned (right) displays. Filled and empty squares refer to with- and without-occluder displays, respectively. Error bars indicate ± 1 standard errors of the mean.

Amount \times Occluder interaction ($F_{2,68} = 19.83$, $p < 0.001$) as well as the main effect of Slant Amount ($F_{2,68} = 4.98$, $p < 0.01$), were significant. As regards the Slant Amount \times Occluder interaction, the slant contrast in without-occluder displays and the slant assimilation in with-occluder displays decreased as $|\theta|$ increased from 10 to 30 deg. This was confirmed by planned comparisons: RES values for without-occluder displays approached zero, representing veridicality, as the simulated slant became larger (0.72 vs. 0.17 for $|\theta| = 10$ vs. 30 deg: $F_{1,34} = 27.95$, $p < 0.001$); a similar, though not significant, tendency was observed in with-occluder displays (-0.62 vs. -0.44 for $|\theta| = 10$ vs. 30 deg: $F_{1,34} = 3.00$, $p = 0.09$).

Consistently with the continuous model of approximation effectiveness, the difference between the amounts of perceived slant for with- vs. without-occluder displays gradually decreased away from $\theta = 0$ in both directions. To evaluate the fit between empirical data and predictions illustrated in Fig. 4 we computed Δ RES, the differences between mean RES values for with- vs. without-occluder displays.

As shown in Fig. 10, the distribution of Δ RES values is consistent with a continuous model of approximation effectiveness of the form $(ax^2 + b)$ [$a = -0.0008$, $b = 1.34$, $df = 4$, $sse = 0.09$, $rmse = 0.15$, adjusted $r^2 = 0.84$]; while it is not fitted by a step-like function of the form $\frac{1}{2}b(\text{sign}(x - a) - \text{sign}(x + a))$ [$20 < a < 30$, $b = 1.1$, $df = 4$, $sse = 1.01$, $rmse = 0.50$, adjusted $r^2 < 0$]. The best-fitting parabola decreases to zero at $|\theta| = 39$ deg.

To evaluate the effect of approximation on perceived slant direction, we analyzed the distribution of sign errors (positive instead of negative, and vice versa, relative to the frontoparallel plane) extracted from observers' slant adjustments. Individual error percentages were computed for each experimental condition. Fig. 11 shows mean error percentages of slant direction judgments as a function of

signed stereo slant for asymmetrically (left) and symmetrically (right) aligned displays. A mixed factorial analysis of variance was performed on arcsin-transformed data (following the same design described for RES). Direction errors were more frequent for decreasing amounts of stereo slant (main effect of Slant Amount: $F_{2,68} = 7.09$, $p < 0.01$), when the occluder was present (main effect of Occluder: $F_{1,34} = 43.73$, $p < 0.001$), and when the upper planar patch was negatively slanted and asymmetrically-aligned (Slant Direction \times Alignment interaction: $F_{2,68} = 6.21$, $p < 0.05$). The significance of the latter interaction was consistent with the expected effect of T-junction information.

5.3. Discussion

First, consider our baseline displays with zero horizontal scale disparity of the upper patch used as a control for the role of pictorial cues in the estimation of stereo slant. Such displays provided observers with at least two kinds of monocular information about slant. First, the compression of a region with respect to a co-axial reference region (in our displays, the horizontal compression of the upper rectangle relative to the lower) could be taken as a foreshortening cue to unsigned slant. Second, in asymmetric displays the combination of foreshortening and T-junctions formed by the gray rectangles and the surrounding black field supported the positive slant of the upper patch. Since the largest horizontal compression led to a significant error in the expected direction, the effect of pictorial cues should be taken into account to evaluate the specific contribution of horizontal scale disparity to slant estimation.

Overall results are consistent with the idea that the misperception of image-specified parts depends on the approximation process involved in limiting cases of amodal completion; while they are inconsistent with the literal representation of positions and orientations of surface patches

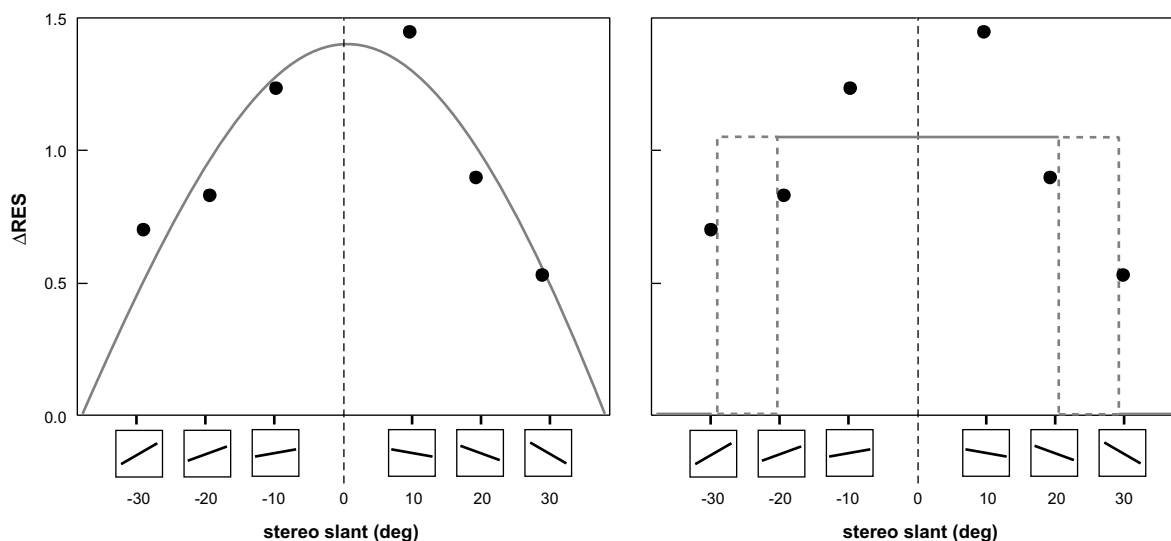


Fig. 10. Fit of Δ RES values by two approximation functions: a parabola (left) vs. a step-like function (right). Each Δ RES value is the signed difference between the mean RES value for without-occluder displays and the mean RES value for with-occluder displays.

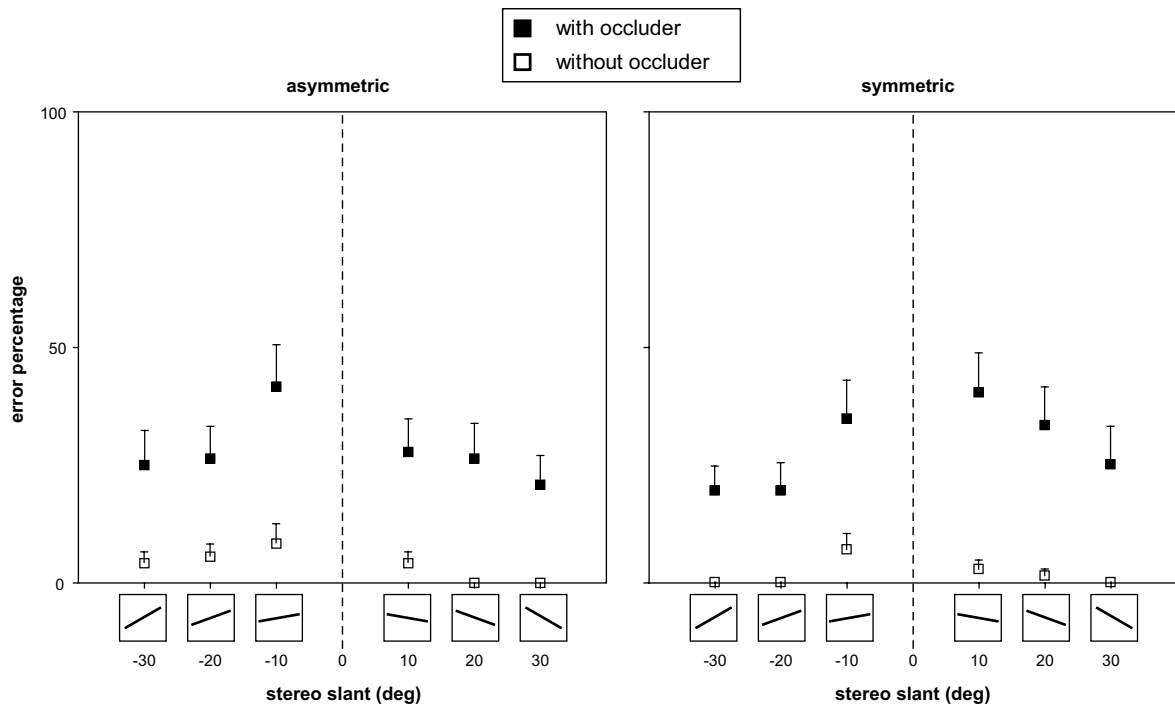


Fig. 11. Percentages of slant-direction errors as a function of stereo slant in with-occluder (filled squares) vs. without-occluder (empty squares) conditions for asymmetrically-aligned (left) and symmetrically-aligned (right) displays.

assumed by conventional interpolation. Approximation distorts image-specified parts towards relatability, resulting in a solution closer to co-planarity (i.e., subtending a lower degree of torsion) that causes the slant assimilation effect. The overestimation of relative slant obtained in without-occluder displays is consistent with the conjoin effect of observing distance on stereo-depth, with an overestimation for small observing distances (Johnston, 1991), and slant contrast, with a repulsion effect between the slant of the two twisted surface patches (Gillam & Blackburn, 1998).

The overall trend of relative estimated slant over twist angle supports the continuous approximation hypothesis: as the twist angle departs from zero, the effectiveness of visual approximation decreases and proportionally reduces the difference between the estimated slant in with- vs. without-occluder displays. The range of twist angles explored in our study allowed us to infer a critical twist value ($|\kappa| = 39$ deg) beyond which approximation is not effective. We view it as the limit for connecting two twisted planar patches by an amodally-completed 3D surface with torsion, at least under these display conditions.

As regards slant direction, the distribution of sign errors extracted from the patterns of adjustments showed that visual approximation also affected sensitivity to direction of twist for some displays. This finding prompted us to use an objective method for measuring twist sensitivity in Experiment 3.

The irrelevance of alignment *per se* is consistent with the idea that approximation depends on the overall (rather than extremal) amount of torsion of the amodal surface connecting the two surface patches.

6. Experiment 2: Relative slant with vs. without an illusory occluder

The difference between displays with and without a real occluder, obtained in Experiment 1, suggested that approximation affects slant perception when the occlusion geometry is near the limits for amodal completion. However, one might argue that the two conditions are not comparable, since the complexity of the two displays is not equivalent and the patterns of luminance and disparity are unbalanced, given that the real occluder involves an additional luminance contour and an additional depth level. To make the two conditions more balanced and to evaluate slant assimilation in displays containing the same elements we ran another experiment, using the same method but contrasting a condition with an *illusory* occluder and one without the occluder, in which the inducing lines were misaligned (Fig. 12).

6.1. Method

6.1.1. Participants

Forty-three undergraduate students of the University of Trieste with normal or corrected-to-normal vision and naive to the purpose of the experiment served as unpaid participants. Five participants were excluded from the experimental session because they failed the screening test for stereoscopic vision, while four of the 38 observers who participated in the experimental session were excluded from the final analysis due to failure to meet the threshold criterion for performance on the experimental task.



Fig. 12. Stimuli used in Experiment 2. Stereograms depict with-occluder (left) and without-occluder (right) symmetric displays with $\theta = 30$ deg.

Observers were randomly assigned to one of the two levels of the between-subjects factor of presence or absence of the occluder.

6.1.2. Apparatus, displays, procedure, and design

The apparatus, the windows, and the two gray rectangular patches were the same as in Experiment 1. The new displays included two black vertical segments (2-pixel thick) flanked on either sides of the two patches, with height, horizontal separation, and disparity identical to those of the vertical sides of the real occluder used in Experiment 1. With- and without-occluder displays differed only in the vertical position of the flanking segments.

In with-occluder displays the two flanking segments were centered with respect to the horizontal axis of the white square background (Fig. 12 left) so to form an illusory rectangular surface occluding a vertically-elongated surface emerging from the amodal completion of the two target patches. The perceptual evidence of the illusory occluder was confirmed by reports of 10 independent observers.

In without-occluder displays the flanking segments were vertically shifted in opposite directions (Fig. 12 right) to align the bottom terminator of the upper segment with the bottom side of the upper patch and the top terminator of the lower segment with the top side of the lower patch. The two combinations of segment positions were balanced within each session.

Other features of the displays (simulated slant, alignments, relative width in baseline conditions, gauge probe), the experimental design, and the procedure were like in Experiment 1.

6.2. Results

First, we analyzed the distribution of raw matched slant values for baseline displays. The analysis of variance with Width (3) and Alignment (2) as within-subjects factors and Occluder (2) as a between-subjects factor showed that both Width ($F_{2,64} = 6.30$, $p < 0.01$) and Occluder ($F_{1,32} = 6.18$, $p < 0.05$) significantly affected slant estimates. The main effect of Width resembled the effect obtained in Experiment 1. Slant estimates for 16%, 8%, 4% horizontally-compressed upper rectangles were 4.46, 0.17, -0.12 deg for asymmetric displays and 0.73, 0.29, -0.78 deg for symmetric displays (4.46 vs. 0: $t = 2.96$,

$df = 33$, one-tailed, $p < 0.01$; while, for the other five contrasts: $t < 1$). We found no consistent explanation for the main effect of Occluder (1.99 vs. -0.41 deg for with- vs. without-occluder displays).

The following analyses reveal that the distributions of AES and RES (Fig. 13), of Δ RES (Fig. 14), and of slant-direction error percentages (Fig. 15), were consistent with approximation-based expectations.

A Slant Amount (3) \times Slant Direction (2) \times Alignment (2) \times Occluder (2) mixed factorial analysis of variance on RES showed the following set of significant effects, that basically replicated the one obtained in Experiment 1: Occluder ($F_{1,32} = 32.33$, $p < 0.001$) with average RES values for with- vs. without-occluder about halved with respect to those in Experiment 1, but always symmetric across the zero and significantly different from it (with-occluder, -0.27 vs. 0: $t = 3.71$, $df = 16$, one-tailed, $p < 0.01$; without-occluder, 0.27 vs. 0: $t = 5.68$, $df = 16$, one-tailed, $p < 0.001$); Slant Direction ($F_{1,32} = 19.43$, $p < 0.01$) with RES values always in the direction of enhancement for positively-slanted displays and attenuation for negatively-slanted displays, independent of Alignment (0.13 vs. -0.09 for positive vs. negative slant, in asymmetric displays; 0.08 vs. -0.12 for positive vs. negative slant, in symmetric displays); Slant Amount ($F_{5,160} = 9.00$, $p < 0.001$), with RES inversely proportional to the absolute amount of stereo slant (average RES were 0.13, -0.03 , -0.11 from the smallest to the largest stereo-slant); Alignment \times Occluder ($F_{1,32} = 5.80$, $p < 0.05$) with a superiority of RES values for asymmetrically- vs. symmetrically-aligned displays, present in the without-occluder condition (0.33 vs. 0.20: $F_{1,32} = 5.85$, $p < 0.05$) but absent in the with-occluder condition (-0.30 vs. -0.24 : $F < 1$); Alignment \times Slant Amount ($F_{2,64} = 4.25$, $p < 0.05$) with a steeper decrease of RES values as a function of absolute slant for asymmetrically- vs. symmetrically-aligned displays.

Although the Slant Amount \times Occluder interaction was not significant ($F_{2,64} = 2.81$, $p = 0.067$), the pattern of slant estimates in Experiment 2 was similar to the one in Experiment 1. Slant contrast in without-occluder displays followed the same trend (0.47 vs. 0.10 for $|\theta| = 10$ vs. 30 deg: $F_{1,32} = 17.44$, $p < 0.001$) and slant assimilation in with-occluder displays was again unaffected by simulated slant (-0.20 vs. -0.32 for $|\theta| = 10$ vs. 30 deg: $F_{1,32} = 1.63$, $p = 0.21$).

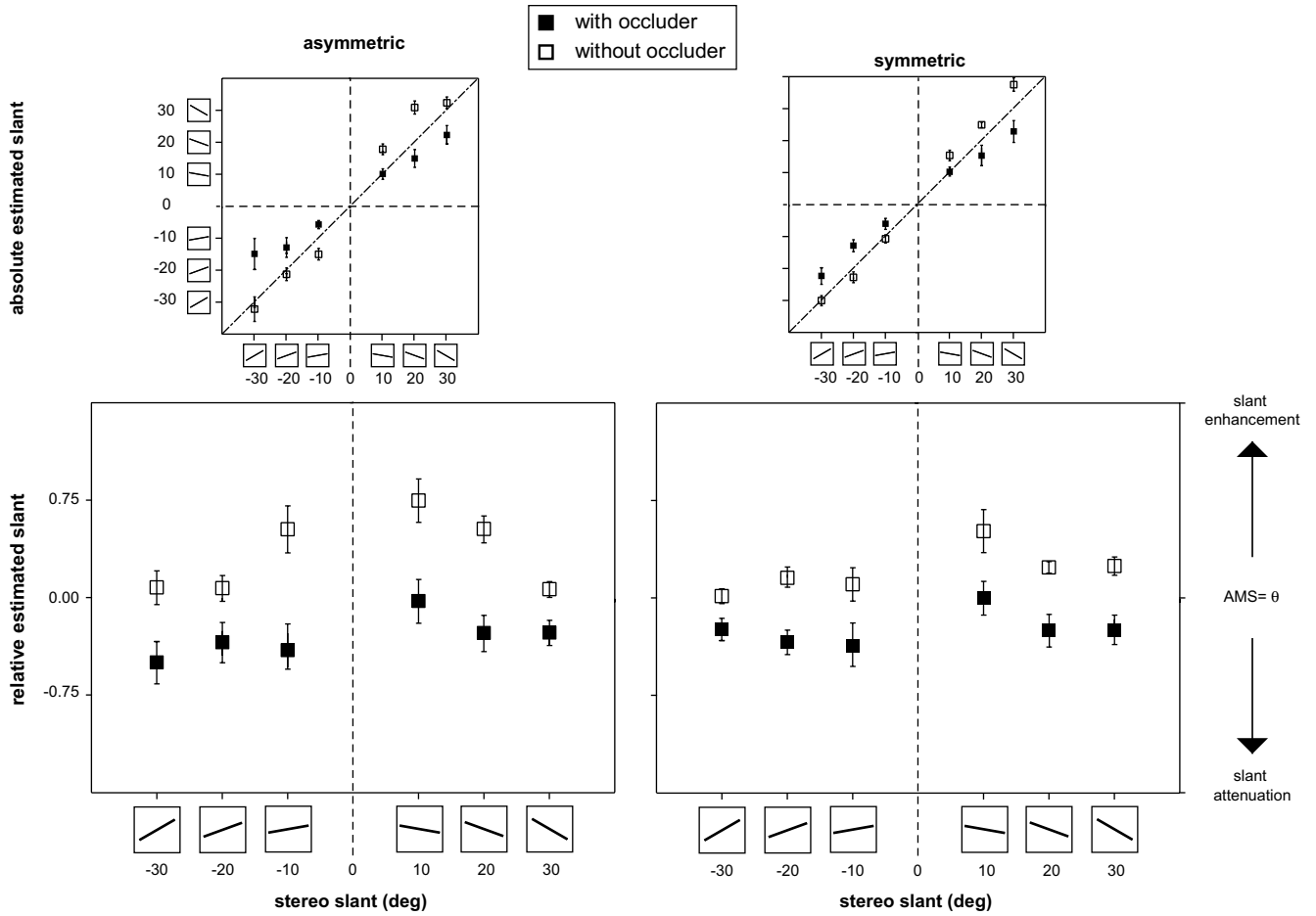


Fig. 13. Mean values of absolute matched slant (top), and relative matched slant (bottom), as a function of the stereo slant of the upper patch, for asymmetrically-aligned (left) and symmetrically-aligned (right) displays. Filled and empty squares refer to with- and without-occluder displays, respectively. Error bars indicate ± 1 standard errors of the mean.

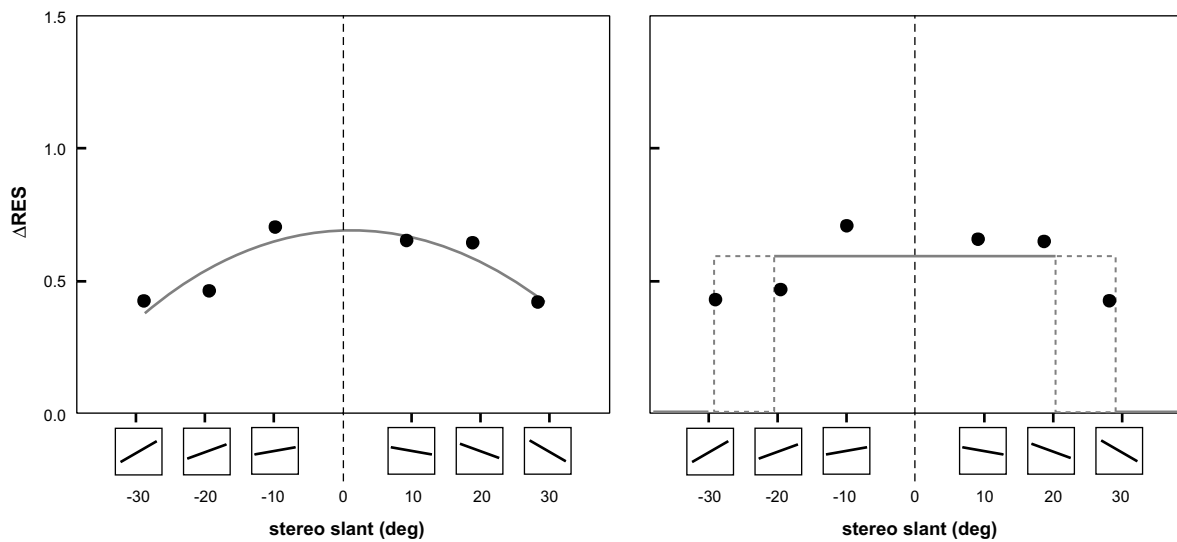


Fig. 14. The pattern of ΔRES values computed from data obtained in Experiment 2 are fitted by two approximation functions: a parabola (left) vs. a step-like function (right).

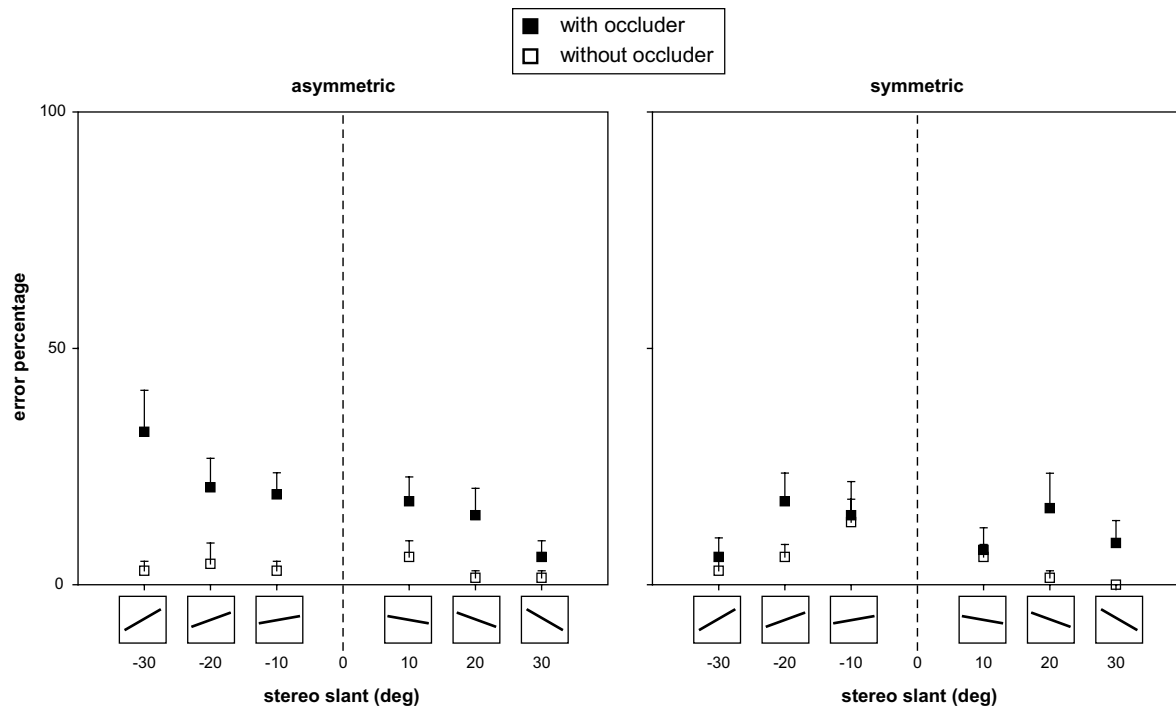


Fig. 15. Error percentage as a function of stereo slant for asymmetrically-aligned (left) and symmetrically-aligned (right) displays. Filled and empty squares refer to with- and without-occluder displays, respectively.

As in Experiment 1 the pattern of Δ RES values was consistent with a continuous model of approximation being shaped as the positive part of a parabola [left graph: $a = -0.0003$, $b = 0.69$, $df = 4$, $sse = 0.02$, $rmse = 0.07$, adjusted $r^2 = 0.77$], rather than as a step-like function [right graph: $20 < a < 30$, $b = 0.61$, $df = 4$, $sse = 0.37$, $rmse = 0.30$, adjusted $r^2 < 0$]. The critical value $|\kappa|$ (corresponding to the zero-crossing) was 47 deg.

Fig. 15 illustrates the distribution of error percentages of slant direction judgments averaged over our experimental conditions. Results of a mixed factorial analysis of variance (following the same design of Experiment 1) showed that direction errors were more frequent when the occluder was present ($F_{1,32} = 7.76$, $p < 0.01$). The pattern of error percentages partially differs from the one in Experiment 1. Direction errors were more frequent in negatively vs. positively slanted displays ($F_{1,32} = 7.30$, $p < 0.05$) and were larger in asymmetrically-aligned than symmetrically-aligned displays when the occluder was present (18% vs. 11%: $F_{1,32} = 15.20$, $p < 0.001$), but not when the occluder was absent (3% vs. 4%: $F < 1$), as confirmed by the significant Alignment \times Occlusion interaction ($F_{1,32} = 12.06$, $p < 0.01$).

6.3. Discussion

The goal of Experiment 2 was to test whether the slant assimilation effect found in Experiment 1 was independent of disparity and luminance differences between displays with and without a real occluder. Results were similar, despite the fact that in Experiment 2 all displays were

equivalent with respect to depth-from-disparity and luminance. This finding supports the idea that, at least when torsion is required to smoothly connect twisted patches, amodal completion is supported by a process of visual approximation that leads to slant assimilation.

Slant assimilation was stronger in Experiment 1 (real vs. no occluder) than in Experiment 2 (illusory vs. no occluder), leading to a smaller $|\kappa|$ value and worse accuracy of slant direction judgments (Experiment 1: RES = -0.50 , $|\kappa| = 39$ deg, % error for with- vs. without-occluder displays = 28.4 vs. 2.8; Experiment 2: RES = -0.27 , $|\kappa| = 47$ deg, % error for with- vs. without-occluder displays = 15.1 vs. 4.0). Such differences could be attributed to the higher probability of amodal completion in real-occluder conditions with respect to illusory-occluder conditions. In Experiment 2 occasional depth reversals occurred and the display was occasionally perceived as a mosaic of regions and line fragments on a homogeneous background.

The consistent pattern of slant estimates for with- vs. without-occluder displays as a function of stereo slant found in Experiments 1 and 2 strongly supports the continuous model of approximation. Approximation is effective when the torsion of the connecting surface is within the limits in which amodal completion does occur.

7. Experiment 3: Discounting the occluder

In principle, the effect of slant assimilation measured in Experiments 1 and 2 might be independent of amodal completion. According to an alternative explanation, the occluder by itself might distort the perceived slant of adjacent

regions. Consistently with Nakayama, Shimojo, and Silverman (1989), when two regions share a border, the near region inhibits the far one by pulling the common border towards the depth level of the near region, producing a regression towards the occluder (Grossberg, 1994). This hypothesis is consistent with previous findings by Häkkinen and Nyman (1997). The authors found that perceived slant of a surface that was horizontally magnified in one eye and adjacent to a binocular wholly specified plane was strongly reduced when the pattern of relative disparity was consistent with partial occlusion relative to when it was not. On the other hand, the occluder might provide a reference frame for slant (Gillam & Blackburn, 1998) and facilitate its veridical estimation.

Since slant assimilation in occlusion conditions might be a composite effect, we carried out an experiment to assess the possible contribution of occluder presence and evaluate the actual effect of approximation. In Experiment 3 we used with-occluder displays in which the unification of the two surface patches was either supported or not by edge geometry. Stimuli included all symmetrically-aligned displays of Experiment 1 plus two new with-occluder displays and two new without-occluder displays. In with-occluder displays, two factors known to be needed for amodal completion were manipulated; the tangent discontinuity at contour junctions (see the junction rounding in Fig. 16 top left) leading to rounded/aligned displays, and the alignment of patch edges (see the misaligned vertical edges in Fig. 16 top right) leading to abrupt/misaligned displays. According to several studies (Lescher & Mingolla, 1993; Palmer, Kellman, & Shipley, 2006; Purghé & Russo, 1999; Shipley & Kellman, 1990) the avoidance of tangent discontinuities in rounded/aligned displays hinders visual completion. Similarly, abrupt/misaligned displays included a horizontal offset between corresponding vertical edges larger than 20 min over which visual completion should not occur (Hilger & Kellman, 2005; Roncato & Casco, 2003; Shipley & Kellman, 1992; Tse, 1999a). Both of these manipulations weaken contour interpolation and surface spreading (Kellman, Garrigan, Yin et al., 2005) according to the idea that surface qualities spread within the bound-

aries of a single perceptually completed surface (Yin et al., 2000). The same manipulations of gray patches were utilized for with- and without-occluder displays.

We used an objective classification method sensitive to object completion (Kellman, Garrigan, Yin et al., 2005) and measured the sensitivity to twist direction. Observers made a speeded judgment of whether the twist of surface patches was *positive* or *negative*. Such a method minimized the role of subjective factors (unavoidable in the adjustment procedure) and allowed us to infer the relationship between slant sensitivity and direct measures of slant assimilation obtained in Experiments 1 and 2.

According to approximation, the performance loss in with- vs. without-occluder displays is larger when surface patches can be amodally completed, regardless of the occluder. Moreover, the continuous approximation model predicts that the amount of loss should decrease as an inverse function of the simulated twist angle. By contrast, any occluder-presence hypothesis predicts a constant performance loss, independent of amodal completion and twist amount.

7.1. Method

7.1.1. Participants

Twenty-three undergraduate students of the University of Trieste with normal or corrected-to-normal vision and naive to the purpose of the experiment served as unpaid participants. Three participants were excluded from the final experimental session: two of them failed the test for stereoscopic slant perception, while one did not reach the reaction time criterion at the end of the training session. The remaining 20 observers participated in all conditions of the experiment, which followed a factorial within-subjects design.

7.1.2. Apparatus and displays

Both the apparatus and the criteria used for stimulus construction were the same as in previous experiments. The computer associated *k* and *l* keys to each allowed response, and recorded response type and reaction time

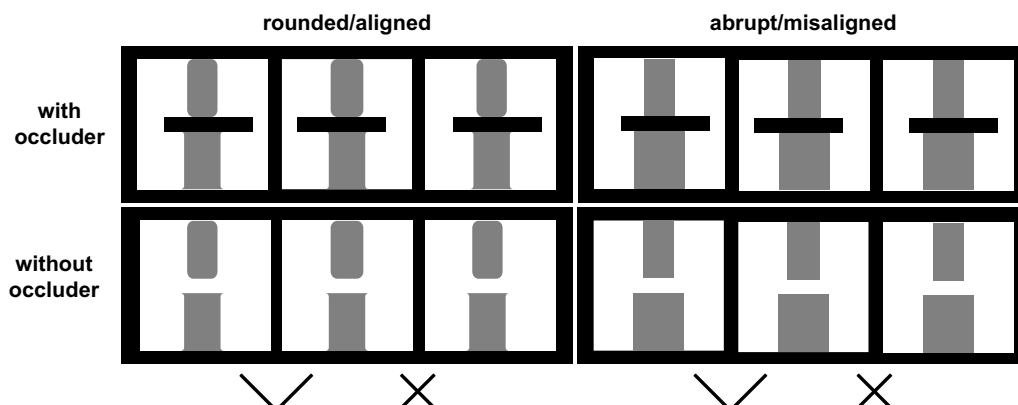


Fig. 16. Displays for rounded/aligned and abrupt/misaligned conditions used in Experiment 3 (with $\theta = 30$ deg). Top and bottom rows illustrate with-occluder and without-occluder conditions. Abrupt/aligned displays were those of Experiment 1 (Fig. 7).

(RT) using PsychToolbox. The association between left (k key) vs. right (l key) and negative vs. positive twist was based on the following type of compatibility stressed by instructions: “Press either the left or right key depending on whether the left or right side of the upper rectangle appears closer to you”. Three amounts of twist angle $|\theta|$ were used: keeping the bottom patch frontoparallel (i.e., $\theta = 0$ deg), $|\theta|$ values were 10, 20, 30 deg. For each $|\theta|$ value we constructed two displays, one with *negative* and the other with *positive* twist.

Three types of patches were selected over the two occlusion conditions, corresponding to three levels of edge geometry:

1. Abrupt/aligned (Fig. 7). Stimuli were the symmetrically-aligned displays of Experiment 1.
2. Rounded/aligned (Fig. 16 left). Stimuli were obtained by slightly modifying the abrupt/aligned displays as follows: (i) the four corners of the lower rectangle were rounded using a concave outward arc of a circle with a 21-min radius; (ii) the four corners of the upper rectangles were rounded using a convex inward arc of ellipse simulating a slanted circular arc with a 21-min radius. The aspect ratio of the arc of ellipse was contingent on the simulated slant of the patch.
3. Abrupt/misaligned (Fig. 16 right). Stimuli were obtained by substituting the lower patch of abrupt/aligned displays with a larger one (subtending a visual angle of 2.44 deg), while keeping the upper patch identical to the one used in the abrupt/aligned-patches condition.

With-occluder displays with rounded/aligned and abrupt/misaligned edges were those in which two basic conditions for completion were not satisfied despite the occluder presence. Patches in without-occluder displays (Fig. 16 bottom) matched those in with-occluder displays in all respects.

The whole stimulus set, shown to each observer, included 36 different displays, resulting from the combination of the three factors used in the experimental design [Twist Angle (10, 20, 30 deg); Edge Geometry (abrupt/aligned, rounded/aligned, abrupt/misaligned); Occluder (with vs. without)], and the balancing variable Twist (positive vs. negative).

7.1.3. Procedure and design

As shown in Fig. 17, any trial included the following steps: (a) a 30-pixel-wide red cross was displayed at the center of the display with a 25.2-min crossed disparity, making it to appear at a depth level midway between the occluder and the frame; (b) when the observer felt to be ready, he/she pressed a key to display the stimulus; (c) the display remained on the screen until one of the two response keys was pressed; (d) after key press a 500-ms mask was displayed and the next trial followed.

Given the individual variability in achieving stereo and the consequent difficulty to fix the exposure time, observers were allowed to control stimulus duration by pressing the response key and were instructed to respond as quickly as possible while watching the display and maintaining an accurate performance. This method deliberately modulates the amount of time in which stimulus information is available and sets the conditions for a trade-off (Gratton, Coles, Sirevaag, Eriksen, & Donchin, 1988; Wickens, 1984; Wickens & Hollands, 2000); i.e., individual data should exhibit an increase in twist sensitivity following from an increase of observation time within each experimental condition, independent of the relative difficulty of the task due to display geometry. The procedure included instructions, the test for stereo vision, training, and the experimental session.

7.1.3.1. Instructions. The experimenter introduced binocular vision, told participants that the experiment involved slant perception, and showed a physical model made of twisted separated cardboards to convey the idea of the displays. Written instructions required participants to respond quickly and to use the red cross to support steady fixation during stimulus presentation.

7.1.3.2. Test for stereo vision. The test was similar to those used in previous experiments.

7.1.3.3. Training. The training session included three blocks of 20 trials with an auditory feedback. During the first block the experimenter collected additional information through participants' verbal reports (displays description, judgment of perceived twist direction and verbalization of

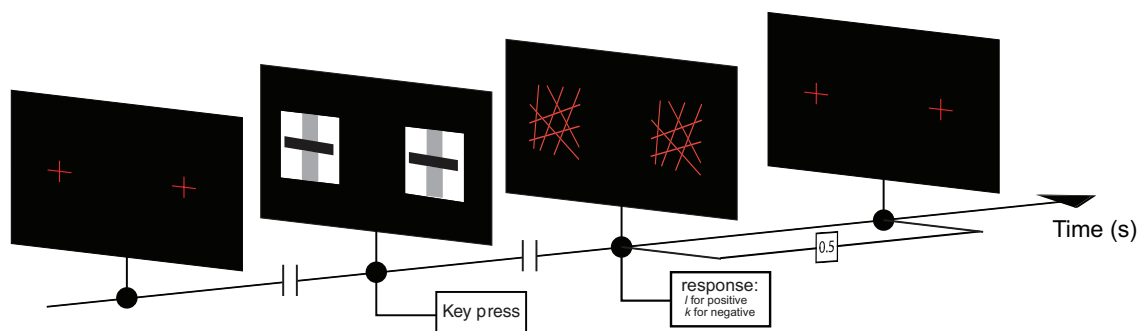


Fig. 17. Temporal sequence illustrating one trial of Experiment 3.

the response key); furthermore, in three trials (one for each stimulus subset, with the 10-deg-twist with-occluder display) participants were asked to report whether they perceived the two surface patches as unified or not. All participants perceived the two patches as separate surfaces in trials with rounded/aligned with-occluder displays; 15 out of 20 in trials with abrupt/misaligned with-occluder displays; and only 4 out of 20 in trials with abrupt/aligned with-occluder displays. This was taken as preliminary evidence that the manipulations used to generate rounded/aligned and abrupt/misaligned displays weakened the completion of the surface patches, although completion processes could be partially activated at low spatial frequencies.

During the remaining blocks participants were required to respond following the standards of the experimental session. Only participants who at the end of the last block met performance criteria (60% correct & faster than 4 s) entered the experimental session.

7.1.3.4. Experimental session. Each observer was given a set of 432 trials without auditory feedback, corresponding to 12 random sequences of the 36 different displays. The only constraint was the avoidance of repetitions of the same display on subsequent trials. The experimental session lasted 50 min and was divided into eight blocks of 54 trials, separated by short rest periods.

7.2. Results

Given the expectation of a trade-off between accuracy and observation time, we performed a preliminary analysis of performance. Within each condition of the Twist Angle (3) × Edge Geometry (3) × Occluder (2) design every response (either correct or wrong) was categorized as fast vs. slow depending on whether the response/observation time, RT , was below or above the median of the condition. Then, two sensitivity values were computed for each condition, one for fast responses (short observation time) and one for slow responses (long observation time). Sensitivity was computed as a d' measure by taking the negative twist as the noise and the positive twist as the signal embedded in noise. Three observers were excluded from subsequent analyses since their performances were characterized by negative values of d' (1, 3, and 4 negative values out of 18, respectively). As expected, the average d' for slow responses was significantly larger than the average d' for fast responses (1.51 vs. 1.34; $t = 3.27$, $df = 305$, two-tailed, $p < 0.01$).

The demonstration of a trade-off between sensitivity and RT convinced us that the individual performance in the twist classification task could be appropriately described by a synthetic measure combining d' and mean RT for correct responses. The rationale for such a measure derives from the commonly held assumption that d' increases as a weighted function of the square root of RT : $d' = k\sqrt{RT}$. Under such an assumption the relationship

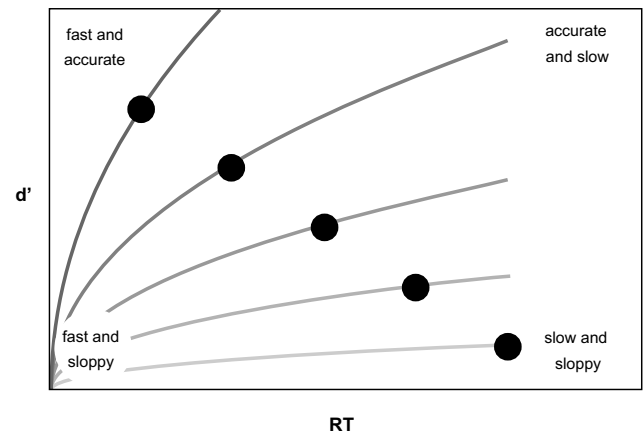


Fig. 18. Isoperformance curves in the $[RT, d']$ space, each resulting from the trade-off between accuracy and response/observation time. Labels in the four corners describe extreme performance types. An overall improvement of performance in a speeded classification task corresponds to a migration from the “slow and sloppy” corner to the “fast and accurate” corner, as shown by points lying on different isoperformance curves. The family of curves displays the function cc , with the k value representing the overall level of performance (dark-to-light gray = large-to-small k).

between d' and RT is represented by a family of half parabolas. Each parabola is an isoperformance curve, with d' increasing as a negatively accelerated function of RT , at a rate proportional to k . Fig. 18 shows a set of $[RT, d']$ points lying on different isoperformance curves: as suggested by Wickens (1984), such a pattern is expected in tasks in which the feature to be detected is relatively poor and response speed is emphasized, as in our speeded classification task. As the detectability of the feature increases, the point describing the overall performance crosses the $[RT, d']$ space from the slow and sloppy corner to the fast and accurate corner. The k coefficient provides a synthetic measure of the performance level: $k = d' \frac{1}{\sqrt{RT}}$ and can be interpreted as a measure of accuracy weighted by the amount of available stimulus information.

Fig. 19 depicts the distribution of d' and mean RT for correct responses in the 18 conditions of the experimental design. Isoperformance curves for different Twist Angle levels were drawn by computing a representative k value derived from an average d' and an average RT for that level. Consistently with the hypothesis that large twist angles are easier to classify: points were arranged along a diagonal, with steepness of the isoperformance curve increasing as the twist angle gets larger. As expected, performance in the twist classification task improved as a function of twist angle for both with- and without-occluder displays independent of Edge Geometry. In general, the pattern of $[RT, d']$ points for without-occluder displays was shifted towards the “fast and accurate” corner relative to the pattern for with-occluder displays, consistently with the hypothesis that the presence of the occluder makes slant less discriminable from the frontal parallel plane and therefore causes a global performance loss.

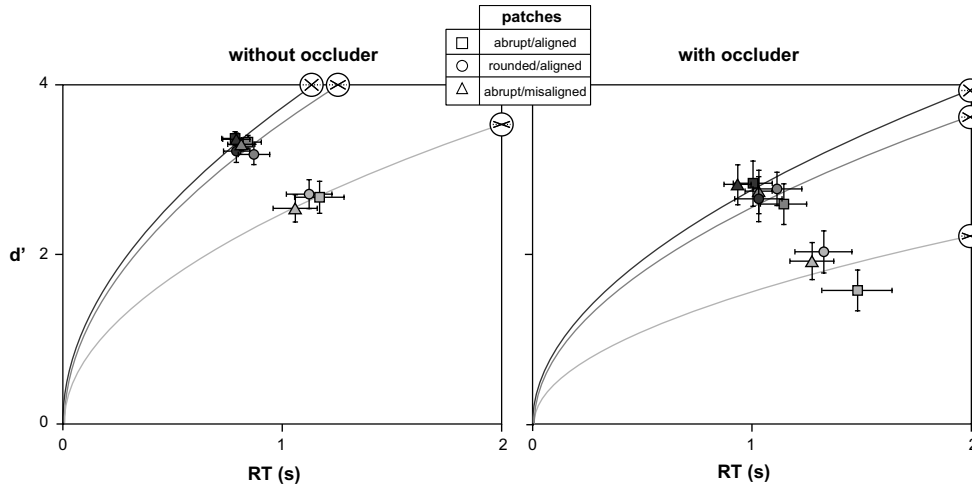


Fig. 19. Performance in the $[RT, d']$ space for without-occluder (left) and with-occluder (right) displays, for the three levels of Twist Angle (dark-to-light symbols representing large-to-small angles) and the three levels of Edge Geometry (coded by symbol shape as shown in the legend).

Performance in abrupt/aligned trials was worse than performance in rounded/aligned and abrupt/misaligned trials (square symbols below the corresponding isoperformance curves, closer to the “slow and sloppy” corner) in the with-occluder condition for 10- and 20-deg twist angles, while no difference was observed in the without-occluder condition. This is consistent with the conclusion that classification performance was not affected by edge geometry *per se*, but by completion. Consistent with the approximation hypothesis, edge geometry was effective only when the occluder was present, setting the conditions for amodal completion.

The results of a repeated-measures analysis of variance on individual k values for each condition of the Twist Angle (3) \times Edge Geometry (3) \times Occluder (2) design supported these observations. For every observer, each k value was computed using the d' and mean RT for correct responses. The main effect of Occluder was significant ($F_{1,16} = 63.88, p < 0.001$): mean $k = 3.42$ vs. 2.51 for without- vs. with-occluder displays. The main effect of Twist Angle was also significant ($F_{2,32} = 101.15, p < 0.01$), with k increasing as a direct function of Twist Angle (mean $k = 3.43, 3.25$, and 2.22 for $|\theta| = 30, 20$, and 10, respectively). Edge Geometry did not produce a significant main effect ($F_{2,32} = 2.38, p = 0.11$), although it interacted significantly with both Occluder ($F_{2,32} = 3.41, p < 0.05$) and Twist Angle ($F_{4,64} = 4.58, p < 0.01$): the mean k for abrupt/aligned displays was smaller than the mean k for the two types of displays in which amodal completion was expected to be weaker, independent of the occluder (2.37 vs. 2.58: $F_{1,16} = 13.31, p < 0.01$); whereas the two k values did not differ in the without-occluder condition (3.44 vs. 3.41: $F < 1$). The significance of the Edge Geometry \times Twist Angle interaction derived from the higher rate of performance loss as a function of twist angle for abrupt/aligned- vs. both rounded/aligned and abrupt/misaligned conditions: the deviation between abrupt/aligned and the other two conditions of edge geometry decreased as a func-

tion of $|\theta|$, approaching zero when $|\theta| = 30$ deg. The mean k for abrupt/aligned displays was smaller than that for rounded/aligned and abrupt/misaligned displays when $|\theta| = 10$ deg (2.04 vs. 2.43: $F_{1,16} = 14.80, p < 0.01$), but neither when $|\theta| = 20$ deg (3.19 vs. 3.40: $F_{1,16} = 1.34, p = 0.26$) nor when $|\theta| = 30$ deg (3.47 vs. 3.51: $F_{1,16} = 1.51, p = 0.23$).

To highlight whether empirical data were consistent with predictions illustrated in Fig. 4, we computed Δk values by taking the difference between each k value in the without-occluder condition and the corresponding k value in the with-occluder conditions, with a performance loss due to occluder presence measured by a positive Δk and vice versa for a negative Δk .

Fig. 20, depicts the distribution of Δk values in the nine conditions of the Twist Angle \times Edge Geometry design.

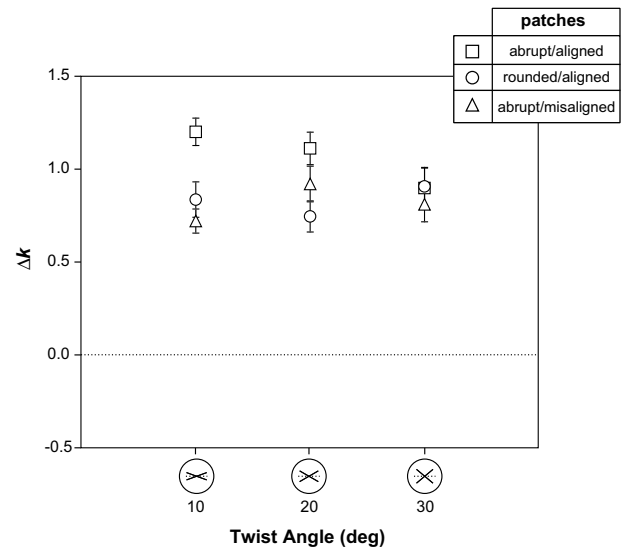


Fig. 20. Mean Δk values as a function of twist angle between surface patches for the three levels of Edge Geometry, coded by symbol shape as shown in the legend. Error bars indicate ± 1 standard errors of the mean.

The presence of the occluder had a clear effect on classification performance: independent of twist angle and Edge Geometry, all Δk values were positive. However, the performance loss due to the occluder was larger for abrupt/aligned displays ($\Delta k = 1.07$) than for rounded/aligned displays ($\Delta k = 0.83$) and abrupt/misaligned displays ($\Delta k = 0.82$). That is, the presence of the occluder had a stronger influence on performance when the shape of surface patches supported amodal completion. The overall amount of performance loss due to the amodal completion component alone was 37% to be compared with the 28% loss due to occlusion (computed on the ratio between Δk and k in the without-occluder condition of rounded/aligned and abrupt/misaligned displays). Furthermore, the pattern of Δk values for abrupt/aligned displays differed from those for both rounded/aligned and abrupt/misaligned displays. Mean Δk values were inversely proportional to $|\theta|$ in the abrupt/aligned condition ($\Delta k = 1.20, 1.11, \text{ and } 0.90$ for $|\theta| = 10, 20, \text{ and } 30$ deg, respectively) while they were nearly constant in rounded/aligned conditions ($\Delta k = 0.84, 0.75, \text{ and } 0.91$, for $|\theta| = 10, 20, \text{ and } 30$ deg, respectively) and in abrupt/misaligned conditions ($\Delta k = 0.72, 0.92, \text{ and } 0.81$ for $|\theta| = 10, 20, \text{ and } 30$ deg). Such a trend is consistent with the continuous model of approximation for abrupt/aligned displays, but neither for rounded/aligned displays nor for abrupt/misaligned.

This was corroborated by the goodness-of-fit analysis in which average Δk values for each edge geometry level were fitted by a parabola of the form ($ax^2 + b$) that provided a good fit for abrupt/aligned displays ($a = -0.0004, b = 1.25, df = 1, sse = 0.00038, rmse = 0.019, \text{ adjusted } r^2 = 0.98$), but not for rounded/aligned displays ($a = 0.00011, b = 0.77, df = 1, sse = 0.0089, rmse = 0.098, \text{ adjusted } r^2 = -0.37$) and abrupt/misaligned displays ($a = 0.00001, b = 0.78, df = 1, sse = 0.017, rmse = 0.13, \text{ adjusted } r^2 = -0.79$). Again, this analysis allowed us to identify a critical value $|\kappa| = 56$ deg.

7.3. Discussion

Results of Experiment 3 suggest that the effect of slant assimilation obtained in Experiments 1 and 2 depends on a combination of occluder presence and completion involving approximation. By itself, occluder presence reduces twist sensitivity and lengthens response time even when the two surface patches cannot be amodally completed. On top of that, the classification task is harder when the two patches become parts of a single partially-occluded surface, as a specific effect of approximation.

Furthermore, the performance loss was affected by the amount of simulated twist only with abrupt/aligned displays, with an inverse relation that resembled the trend of ΔRES as a function of simulated slant measured in Experiments 1 and 2. Such an outcome strongly supports the continuous model of approximation described in Fig. 4.

As regards the critical values $|\kappa|$ obtained in the three experiments (39 deg in Experiment 1, 47 deg in Experiment

2, and 56 in Experiment 3), we attribute the differences to different stimuli, methods, and tasks used to evaluate perceptual performance in the various conditions.

8. Conclusions

We presented three experiments on an effect first reported by Fantoni et al. (2004, 2005) in which amodal completion affects stereoscopic slant. Consider a stereo display simulating two rectangular patches, the one below frontoparallel and the one above slanted around the vertical axis. When the display includes a foreground frontoparallel surface, either real (Experiment 1) or illusory (Experiment 2), and the two patches are amodally completed, their relative slant is underestimated with respect to a baseline condition in which the display does not include the occluder and the two patches are perceived as separate rectangles. In Experiment 3 we demonstrated that such effect includes two components: one attributable to the occluder *per se* (explaining why twist classification is harder in with-occluder displays incompatible with amodal completion because of their edge geometry than in without-occluder displays) and the other contingent on the amodal completion of surface patches (explaining why twist classification of with-occluder displays is harder when edge or junction geometry is compatible with amodal completion, rather than incompatible). Taken together, results support the existence of a specific effect of *slant assimilation from amodal completion*.

Data from Liu and Schor (2005) support the robustness of such an effect. Their work converges with our results, despite important differences in method, displays, and experimental manipulations. First, Liu and Schor obtained the slant assimilation by asking observers to directly estimate the slant of a central patch located between two aligned patches and viewed through an aperture in an untextured occluder. Second, they produced an indirect proof that the slant assimilation also occurs in displays containing strong monocular slant cues (such as the horizontal compression and shape deformation of half-disks specified by a random-dot texture). Third, they concluded that the slant assimilation was not influenced by the amount of crossed disparity of the occluder and by its slant around the vertical axis.

Complementing these findings, our experiments showed that slant assimilation occurs: (a) when fully-specified untextured patches are used, instead of textured patches viewed through apertures; (b) when only one reference surface is available, instead of two (implying the generation of two amodal surfaces); (c) in displays where slant is specified by horizontal scale disparity and not by horizontal point disparity; (d) independent of the occluder (either real or illusory) and the amount of extremal torsion of the connecting surface (since asymmetrically- and symmetrically-aligned displays did not differ). Furthermore, we showed that amodal completion affects slant matching (our Experiments 1 and 2; Liu & Schor, 2005) as well as performance

in an objective classification task (Experiment 3), and that slant assimilation is reduced by rounding the corners of the patches or misaligning their edges (manipulations that make amodal completion less likely), bolstering the view that completion effects are involved in the slant assimilation.

Slant assimilation from amodal completion is relevant for both a broader view of stereopsis and a better understanding of visual completion. As regards stereopsis, such an effect (together with others) supports the idea that the solution of the binocular correspondence problem involves global processes beyond point-by-point matching (Anderson & Nakayama, 1994; Bacon & Mamassian, 2002; Gillam & Borsting, 1988; Nakayama & Shimojo, 1990; Ramachandran & Cavanagh, 1985; Yin et al., 2000). Slant assimilation from amodal completion demonstrates that stereo vision can be influenced by the output of 3D completion processes, consistently with the idea that 3D amodally-completed parts can be generated in parallel with the computation of disparity-defined properties, and modulate them through feedforward interactions (Hoff & Ahuja, 1989; Lee, Medioni, & Mordohai, 2002). This view seems consistent with neurophysiological evidence demonstrating that completion mediated by stereoscopic T-junctions might be supported in early stages of visual processing such as those in V1 cortex (Sugita, 1999) and suggests that models of stereoscopic depth perception that do not include amodal completion as a contributing factor should be updated (Archie & Mel, 2000; De Angelis, Ohzawa, & Freeman, 1991; Grossberg, 1994; Jones & Malik, 1992; Julesz, 1971; Marr & Poggio, 1979; Pollard, Mayhew, & Frisby 1985).

Our results on the misperception of surface patches strongly support approximation as the process underlying visual completion. Approximation leads to a *non-literal* representation of input fragments (rather than *literal* as may usually be assumed by interpolation models), to maximize the conformity to geometric constraints on visual completion: when the smooth connection of non-coplanar patches requires torsion, their representation is regularized towards co-planarity. Such a tendency is comparatively reduced as the amount of torsion required for amodal completion gets bigger, suggesting that approximation acts only within specific tolerance limits, beyond which the patches are perceived as separated, and apparently depends on the overall, rather than extremal, amount of torsion. Although approximation can be considered as stretching the limits of visual completion, it can be equally well described as effects of completion constraints on the representation of spatial inputs. Were there no geometric constraints, there would be no need to adjust the spatial positions of input fragments to conform to them.

The approximation notion is compatible with the modified weak fusion framework (Landy, Maloney, Johnston, & Young, 1995; Young, Landy, & Maloney, 1993). Visual completion of surfaces with different 3D orientations might activate not only the *promotion* of missing information but also the *modification* of weakly-specified parameters like

relative slant. Also within this framework the slant assimilation of amodally-completed input fragments should depend on the amount of discrepancy between local slant-from-disparity and the required degree of torsion.

Relative to interpolation, approximation explains a broader class of completion phenomena, such as slant assimilation and other effects of occlusion on position, shape, and depth of image-specified parts (Fantoni & Gerbino, 2002; Gerbino, 1978; Hou et al., 2006; Liu et al., 1999; Liu & Schor, 2005; Mussap & Levi, 1995).

In general, a computational model of visual completion might include approximation in the following way. Input fragments activate a process that generates a family of solutions (corresponding to completed objects of variable complexity) more or less deviating from locally-specified positions and orientations. The selection of the perceived solution depends on the minimization of the weighted combination of the complexity of the generated object and the amount of deviation from input topography.

On the basis of present results we cannot determine the weights of different components that affect approximation, such as the complexity of amodal parts and various dimensions of deviation from the input. Further studies are needed to reveal the relationships between completion, approximation, and misperception of image-specified parts. As a provisional statement, we claim that visual approximation constitutes a mid-level heuristic supporting the completion of input fragments even in limiting cases of occlusion.

Acknowledgements

The authors gratefully acknowledge supports from: US National Eye Institute Grant EY13518 to PJK; Grant PRIN 2005119851 to WG; Fulbright (CIES) Award to CF.

References

- Anderson, B. L., & Nakayama, K. (1994). Towards a general theory of stereopsis: Binocular matching, occluding contours, and fusion. *Psychological Review*, *101*, 414–445.
- Archie, K. A., & Mel, B. W. (2000). A model for intradendritic computation of binocular disparity. *Nature Neuroscience*, *3*, 54–63.
- Bacon, B. A., & Mamassian, P. (2002). Amodal completion and the perception of depth without binocular correspondence. *Perception*, *31*, 1037–1045.
- Clark, W. C., Smith, A. H., & Rabe, A. (1956). Retinal gradients of outline distortion and binocular disparity as stimuli for slant. *Canadian Journal of Psychology*, *10*, 77–81.
- Cutting, J. E., & Millard, R. T. (1984). Three gradients and the perception of flat and curved surfaces. *Journal of Experimental Psychology: General*, *113*, 198–216.
- da Pos, O., & Zambianchi, E. (1996). *Visual illusions and effects—illusioni ed effetti visivi*. Milano: Guerini e Ass.
- De Angelis, G. C., Ohzawa, I., & Freeman, R. D. (1991). Depth is encoded in the visual cortex by a specialized receptive field structure. *Nature*, *352*, 156–159.
- Fantoni, C., & Gerbino, W. (2001). Probing the amodal completion of asymmetrically occluded angles: A test of interpolation models. *Journal of Vision*, *1*(3), 461–461a. Available from <http://journalofvision.org/1/3/461/>, doi:10.1167/1.3.461.

- Fantoni, C., & Gerbino, W. (2002). A wave-function integration of absolute and relative metric information in visual interpolation. *Journal of Vision*, 2(7), 484–484a. Available from <http://journalofvision.org/2/7/484/>, doi:10.1167/2.7.484.
- Fantoni, C., & Gerbino, W. (2003). Contour interpolation by vector-field combination. *Journal of Vision*, 3(4), 4, 281–303. Available from <http://journalofvision.org/3/4/4/>, doi:10.1167/3.4.4.
- Fantoni, C., Bertamini, M., & Gerbino, W. (2005). Contour curvature polarity and surface interpolation. *Vision Research*, 45, 1047–1062.
- Fantoni, C., Gerbino, W., & Kellman, P. J. (2004). Approximation, torsion, and amodally-unified surfaces. *Journal of Vision*, 4(8), 726a. Available from <http://journalofvision.org/4/8/726/>, doi:10.1167/4.8.726.
- Fantoni, C., Gerbino, W., & Kellman, P. J. (2005). Amodal unification of surfaces with torsion requires visual approximation. *Perception Supplement*, 34, 43.
- Fantoni, C., Gerbino, W., & Rigutti, S. (2007). Form misorientation in limiting cases of amodal completion. *Perception Supplement*, 36, 106.
- Fantoni, C., Hilger, J. D., Gerbino, W., & Kellman, P. J. (submitted for publication). Surface interpolation and 3D relatability. *Journal of Vision*.
- Feldman, J., & Singh, M. (2005). Information along contours and object boundaries. *Psychological Review*, 112, 243–252.
- Fiorani, M., Jr., Rosa, M. G. P., Gattas, R., & Rocha-Miranda, C. E. (1992). Dynamic surrounds of receptive fields in primate striate cortex: A physiological basis for perceptual completion. *Proceedings of the National Academy of Science of the United States of America*, 89, 8547–8551.
- Freeman, R. B. (1966). Absolute threshold for visual slant: The effect of stimulus size and retinal perspective. *Journal of Experimental Psychology*, 71, 170–176.
- Gerbino, W. (1978). Some observations on the formation of angles in amodal completion. *Italian Journal of Psychology*, 2, 85–100.
- Gerbino, W., Scomersi, S., & Fantoni, C. (2006). Amodal completion enhances the discrimination of Vernier offset. *Journal of Vision*, 6(6), 99–99a. Available from <http://journalofvision.org/6/6/99/>, doi:10.1167/6.6.99.
- Gerbino, W., & Fantoni, C. (2006). Visual interpolation is not scale invariant. *Vision Research*, 46, 3142–3159.
- Gillam, B. (1968). Perception of slant when perspective and stereopsis conflict: Experiments with aniseikonic lenses. *Journal of Experimental Psychology*, 78, 299–305.
- Gillam, B., & Blackburn, S. (1998). Surface separation decreases stereoscopic slant but a monocular aperture increases it. *Perception*, 27, 1267–1286.
- Gillam, B., & Borsting, E. (1988). The role of monocular regions in stereoscopic displays. *Perception*, 17, 603–608.
- Gillam, B., & Pianta, M. J. (2005). The effect of surface placement and surface overlap on stereo slant contrast and enhancement. *Vision Research*, 45, 3083–3095.
- Gillam, B., Chambers, D., & Russo, T. (1988). Postfusional latency in stereoscopic slant perception. *Journal of Experimental Psychology: Human Perception and Performance*, 14, 163–175.
- Gillam, B., Flagg, T., & Finlay, D. (1984). Evidence for disparity change as the primary stimulus for stereoscopic processing. *Perception and Psychophysics*, 36, 559–564.
- Gratton, G., Coles, M. G. H., Sirevaag, E., Eriksen, C. W., & Donchin, E. (1988). Pre- and post-stimulus activation of response channels: A psychophysiological analysis. *Journal of Experimental Psychology: Human Perception and Performance*, 9, 793–810.
- Grossberg, S. (1994). 3D vision and figure-ground separation by visual cortex. *Perception and Psychophysics*, 55, 48–120.
- Guttman, S. E., Sekuler, A. B., & Kellman, P. J. (2004). Temporal variations in visual completion: A reflection of spatial limits?. *Journal of Experimental Psychology: Human Perception and Performance* 29, 1211–1227.
- Häkkinen, J., & Nyman, G. (1997). Occlusion constraints and stereoscopic slant. *Perception*, 26, 29–38.
- Hilger, J. D., & Kellman, P. J. (2005). Tolerance for misalignment in contour interpolation: Retinal or relational? *Journal of Vision*, 5(8), 571–571a. Available from <http://journalofvision.org/5/8/571/>, doi:10.1167/5.8.571.
- Hillis, J. M., Watt, S. J., Landy, M. S., & Banks, M. S. (2004). Slant from texture and disparity cues: Optimal cue combination. *Journal of Vision*, 4(12), 1, 967–992. Available from <http://journalofvision.org/4/12/1/>, doi:10.1167/4.12.1.
- Hoff, W., & Ahuja, N. (1989). Surfaces from stereo: Integrating feature matching, disparity estimation, and contour detection. *IEEE Transactions on Pattern Analysis and Machine Intelligence*, 11, 121–136.
- Horn, B. K. P. (1981). *The curve of least energy*. Cambridge: MIT Press.
- Hou, F., Lu, H., Zhou, Y., & Liu, Z. (2006). Amodal completion impairs stereoacuity discrimination. *Vision Research*, 46, 2061–2068.
- Johnston, E. B. (1991). Systematic distortion of shape from stereopsis. *Vision Research*, 31, 1351–1360.
- Jones, J., & Malik, J. (1992). A computational framework for determining stereo correspondence from a set of linear spatial filters. *Image and Vision Computing*, 10, 699–708.
- Julesz, B. (1971). *Foundations of cyclopean perception*. Chicago: University of Chicago Press.
- Kaneko, H., & Howards, I. (1996). Relative size disparities and the perception of surface slant. *Vision Research*, 36, 2505–2517.
- Kanizsa, G., & Gerbino, W. (1982). Amodal completion: Seeing or thinking? In J. Beck (Ed.), *Organization and representation in perception*. Hillsdale, NJ: LEA.
- Kellman, P. J. (2003). Interpolation processes in the visual perception of objects. *Neural Networks*, 16, 915–923.
- Kellman, P. J., & Shipley, T. F. (1991). A theory of visual interpolation in object perception. *Cognitive Psychology*, 23, 141–221.
- Kellman, P. J., Garrigan, P., & Shipley, T. F. (2005). Object interpolation in three dimensions. *Psychological Review*, 112, 586–609.
- Kellman, P. J., Garrigan, P., Yin, C., Shipley, T., & Machado, L. (2005). 3D interpolation in object perception: Evidence from an objective performance paradigm. *Journal of Experimental Psychology: Human Perception and Performance*, 31, 558–583.
- Kellman, P. J., Yin, C., & Shipley, T. F. (1998). A common mechanism for illusory and occluded object completion. *Journal of Experimental Psychology: Human Perception and Performance*, 24, 859–869.
- Koffka, K. (1935). *Principles of Gestalt psychology*. New York: Harcourt Brace.
- Landy, M. S., Maloney, L. T., Johnston, E. B., & Young, M. (1995). Measurement and modeling of depth cue combination: In defense of weak fusion. *Vision Research*, 35, 389–412.
- Lee, M., Medioni, G., & Mordohai, P. (2002). Inference of segmented overlapping surfaces from binocular stereo. *IEEE Transactions on Pattern Analysis and Machine Intelligence*, 24, 824–837.
- Lescher, G. W., & Mingolla, E. (1993). The role of edges and line-ends in illusory contour formation. *Vision Research*, 33, 2253–2270.
- Li, C. Y., & Li, W. (1994). Extensive integration field beyond the classical receptive field of cat's striate cortical neurons-classification and tuning properties. *Vision Research*, 34, 2337–2355.
- Liu, B., & Schor, C. M. (2005). Effects of partial occlusion on perceived slant difference. *Journal of Vision*, 5(11), 4, 969–982. Available from <http://journalofvision.org/5/11/4/>, doi:10.1167/5.11.4.
- Liu, Z., Jacobs, D. W., & Basri, R. (1999). The role of convexity in perceptual completion: Beyond good continuation. *Vision Research*, 39, 4244–4257.
- Marr, D. (1982). *Vision*. San Francisco: Freeman.
- Marr, D., & Poggio, T. (1979). A computational theory of human stereo vision. *Proceedings of the Royal Society of London*, 204, 301–328.
- Massironi, M. (1988). A new visual problem: Phenomenic folding. *Perception*, 17, 681–694.
- Massironi, M., & Sambin, M. (1983). Ondulazione fenomenica: un altro effetto del completamento amodale. *Ricerche di Psicologia*, 26, 205–220.
- Metzger, W. (1954) *Psychologie*. Steinkopff (1st ed., 1941). Spanish translation: *Psicologia*, 1954, Editorial Nova. Italian translation: *I fondamenti della psicologia della Gestalt*, 1963, Firenze, Giunti-Barbera.

- Michotte, A., Thinès, G., & Crabbé, G. (1964). *Les compléments amodaux des structures perceptives*. Louvain: Publications Universitaires.
- Mussap, A. J., & Levi, D. M. (1995). Amodal completion and vernier acuity: Evidence of 'top-but-not-very-far-down' processes. *Perception*, 24, 1021–1048.
- Nakayama, K., & Shimojo, S. (1990). Da Vinci stereopsis: Depth and subjective occluding contours from unpaired image points. *Vision Research*, 30, 1811–1825.
- Nakayama, K., Shimojo, S., & Silverman, G. H. (1989). Stereoscopic depth: Its relation to image fragmentation, grouping, and the recognition of occluded objects. *Perception*, 18, 55–68.
- Palmer, E. M., Kellman, P. J., & Shipley, T. F. (2006). A theory of dynamic occluded and illusory object perception. *Journal of Experimental Psychology: General*, 135, 513–541.
- Pao, H. K., Geiger, D., & Rubin, N. (1999). Measuring convexity for figure/ground separation. In *7th IEEE international conference on computer vision*, Kerkyra, Greece.
- Pelli, D. G. (1997). The VideoToolbox software for visual psychophysics: Transforming numbers into movies. *Spatial Vision*, 10, 437–442.
- Pierce, B. J., & Howards, I. (1997). Types of size disparity and the perception of surface slant. *Perception*, 26, 1503–1517.
- Pollard, S. B., Mayhew, J. E. W., & Frisby, J. P. (1985). A stereo correspondence algorithm using a disparity gradient limit. *Perception*, 14, 449–470.
- Purghé, F., & Russo, A. (1999). Figure anomala e profilo dei contorni inducenti. *Giornale italiano di Psicologia*, 26, 547–565.
- Ramachandran, V. S., & Cavanagh, P. (1985). Subjective contours capture stereopsis. *Nature*, 317, 527–530.
- Rock, I. (1983). *The Logic of Perception*. Cambridge, Massachusetts: MIT Press.
- Roncato, S., & Casco, C. (2003). The influence of contrast and spatial factors in the perceived shape of boundaries. *Perception and Psychophysics*, 65, 1252–1272.
- Saidpour, A., Braunstein, M. L., & Hoffman, D. D. (1994). Interpolation across surface discontinuities in structure-from-motion. *Perception and Psychophysics*, 55, 611–622.
- Sha'shua, A., & Ullman, S. (1988). Structural saliency: The detection of globally salient structures using a locally connected network. In *Proceedings of the international conference on computer vision (ICCV)*.
- Shipley, T. F., & Kellman, P. J. (1990). The role of discontinuities in the perception of subjective figures. *Perception and Psychophysics*, 48, 259–270.
- Shipley, T. F., & Kellman, P. J. (1992). Perception of partly occluded objects and illusory figures: Evidence for an identity hypothesis. *Journal of Experimental Psychology: Human Perception and Performance*, 18, 106–120.
- Singh, M., & Hoffman, D. (1999). Completing visual contours: The relationship between reliability and minimizing inflections. *Perception and Psychophysics*, 61, 943–951.
- Stevens, K. A. (1981). The information content of texture gradients. *Biological Cybernetics*, 42, 95–105.
- Stevens, K. A., & Brookes, A. (1988). Integrating stereopsis with monocular interpretations of planar surfaces. *Vision Research*, 28, 371–386.
- Sugita, Y. (1999). Grouping of image fragments in primary visual cortex. *Nature*, 401, 269–272.
- Takeichi, H., Nakazawa, H., Murakami, I., & Shimojo, S. (1995). The theory of curvature constraint line for amodal completion. *Perception*, 24, 373–389.
- Tse, P. U. (1999a). Complete mergeability and amodal completion. *Acta Psychologica*, 102, 165–201.
- Tse, P. U. (1999b). Volume completion. *Cognitive Psychology*, 39, 37–68.
- Ullman, S. (1976). Filling-in the gaps: The shape of subjective contours and a model for their generation. *Biological Cybernetics*, 25, 1–6.
- Ullman, S. (1996). *High-level vision: Object recognition and visual cognition*. Cambridge, MA: MIT Press.
- van Ee, R., & Erkelens, C. J. (1995). Binocular perception of slant about oblique axes relative to a visual frame of reference. *Perception*, 24, 299–314.
- van Ee, R., van Dam, L. C. J., & Erkelens, C. J. (2002). Bi-stability in perceived slant when binocular disparity and monocular perspective specify different slants. *Journal of Vision*, 2(9), 2, 597–607. Available from <http://journalofvision.org/2/9/2/>, doi:10.1167/2.9.2.
- Wallach, H., & Lindauer, J. (1962). On the definition of retinal disparity. *Psychologische Beiträge*, 6, 521–530. Reprinted in *Hans Wallach On Perception*. New York: Quadrangle, 1976.
- Wickens, C. D. (1984). Processing resources in attention. In R. Parasuraman & R. Davis (Eds.), *Varieties of attention*. New York: Academic Press.
- Wickens, C. D., & Hollands, J. G. (2000). *Engineering psychology and human performance* (3rd ed.). Upper Saddle River: Prentice-Hall Inc.
- Yin, C., Kellman, P. J., & Shipley, T. F. (1997). Surface completion complements boundary interpolation. *Perception*, 26, 1459–1479.
- Yin, C., Kellman, P. J., & Shipley, T. F. (2000). Surface integration influences depth discrimination. *Vision Research*, 40, 1969–1978.
- Young, M. J., Landy, M. S., & Maloney, L. T. (1993). A perturbation analysis of depth perception from combinations of texture and motion cues. *Vision Research*, 33, 2685–2696.
- Youngs, W. M. (1976). The influence of perspective and disparity cues on the perception of slant. *Vision Research*, 16, 79–82.
- Zanforlin, M. (1982). Figural organization and binocular interaction. In J. Beck (Ed.), *Organization and representation in perception* (pp. 251–267). Hillsdale, NJ: Erlbaum.